

1 Heavy Fermions and the Kondo Lattice: A 21st Century Perspective

Piers Coleman

Center for Materials Theory, Rutgers University

136 Frelinghuysen Road, Piscataway NJ 08854, USA

Contents

1 Heavy electrons	2
1.1 Introduction	2
1.2 Local moments and the Kondo effect	2
1.3 The Kondo lattice	6
2 Kondo insulators: the simplest heavy fermions	10
3 Large-N expansion for the Kondo Lattice	11
3.1 Philosophy and formulation	11
3.2 Mean-field theory	16
3.3 Free energy and saddle point	18
3.4 The composite nature of the f -electron	21
3.5 Cooper pair analogy	22
4 Heavy-fermion superconductivity	23
4.1 Symplectic spins and $SP(N)$	24
4.2 Superconductivity in the Kondo-Heisenberg model	25
5 Topological Kondo insulators	27
6 Coexisting magnetism and Kondo effect	30

1 Heavy electrons

1.1 Introduction

In a world where it is possible to hold a levitated high-temperature superconductor in the palm of one's hand, it is easy to forget the ongoing importance of low-temperature research. Heavy-electron materials are a class of strongly correlated electron material containing localized magnetic moments that, by entangling with the surrounding electrons, profoundly transform the metallic properties. A heavy-fermion metal can develop electron masses 1000 times that of copper; it can also develop unconventional superconductivity, transform into new forms of quantum order, exhibit quantum critical and topological behavior. Although most of these properties develop well below the boiling point of nitrogen, the diversity and highly tunable nature of their ground states make them an invaluable work-horse for exploring and researching the emergent properties of correlated quantum matter.

This lecture will give an introduction to heavy-fermion materials, trying to emphasize a 21st century perspective. More extensive discussion and development of the ideas in these notes can be found in an earlier review article [1] and the later chapters of my book *Introduction to Many-Body Physics* [2].

In the periodic table, the most strongly interacting electrons reside in orbitals that are well localized. In order of increasing localization, partially filled orbitals are ordered as follows:

$$5d < 4d < 3d < 5f < 4f. \quad (1)$$

In addition, when moving along a row of the periodic table, the increasing nuclear charge pulls the orbitals towards the nucleus. These trends are summarized in the *Kmetko-Smith diagram* [3], which is shown in Fig 1. The *d*-orbital metals at the bottom left of this diagram are highly itinerant and exhibit conventional superconductivity. By contrast, in rare earth and actinide metals towards the top right-hand corner, the *f*-shell electrons are localized, forming magnets or antiferromagnets. It is the materials that lie in the cross-over between these two regions that are particularly interesting, for these materials are “on the brink of magnetism.” It is in this cross-over region that many strongly correlated materials reside: It is here for instance that we find cerium and uranium, which are key atoms for a wide range of *4f* and *5f* heavy-electron materials.

1.2 Local moments and the Kondo effect

Heavy-electron materials contain a lattice of localized electrons immersed in a sea of mobile conduction electrons. To understand their physics, we need to first step back and discuss individual localized moments and the mechanism by which they interact with the surrounding conduction sea.

The key feature of a localized moment is that the Coulomb interaction has eliminated the high-frequency charge fluctuations, leaving behind a low-energy manifold of degenerate spin states. In rare earth and actinide ions, the orbital and spin angular momentum combine into a single

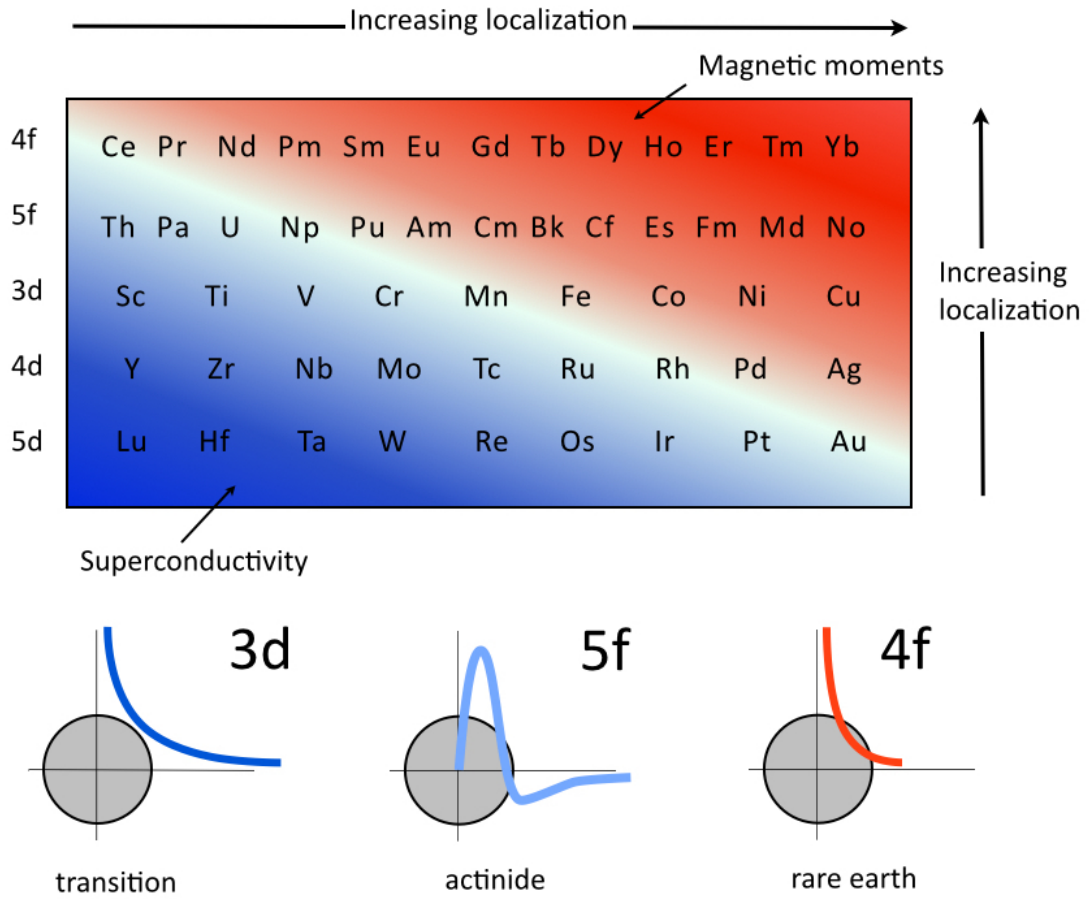


Fig. 1: The Kmetko-Smith diagram [3], showing the broad trends towards increasing electron localization in the d- and f-electron compounds.

entity with angular momentum $\vec{j} = \vec{l} + \vec{s}$. For example, a Ce^{3+} ion contains a single unpaired 4f-electron in the state $4f^1$, with $l = 3$ and $s = 1/2$. Spin-orbit coupling gives rise to a low-lying multiplet with $j = 3 - \frac{1}{2} = \frac{5}{2}$, consisting of $2j + 1 = 6$ degenerate orbitals $|4f^1 : Jm\rangle$, ($m_J \in [-\frac{5}{2}, \frac{5}{2}]$) with an associated magnetic moment $M = 2.64 \mu_B$. In a crystal, the $2j + 1$ -fold degeneracy of such a magnetic ion is split, and provided there are an odd number of electrons in the ion, the Kramers theorem guarantees that the lowest lying state has at least a two-fold degeneracy (Fig. 2 a and b).

One of the classic signatures of localized moments is a high-temperature Curie-Weiss susceptibility, given by

$$\chi \approx \frac{M^2}{3(T + \theta)} n_i \quad M^2 = g^2 \mu_B^2 j(j + 1), \quad (2)$$

where n_i is the concentration of magnetic moments, while M is the magnetic moment with total angular momentum quantum number j and gyromagnetic ratio g (g -factor). θ is the Curie-Weiss temperature, a phenomenological scale that takes account of interactions between spins.

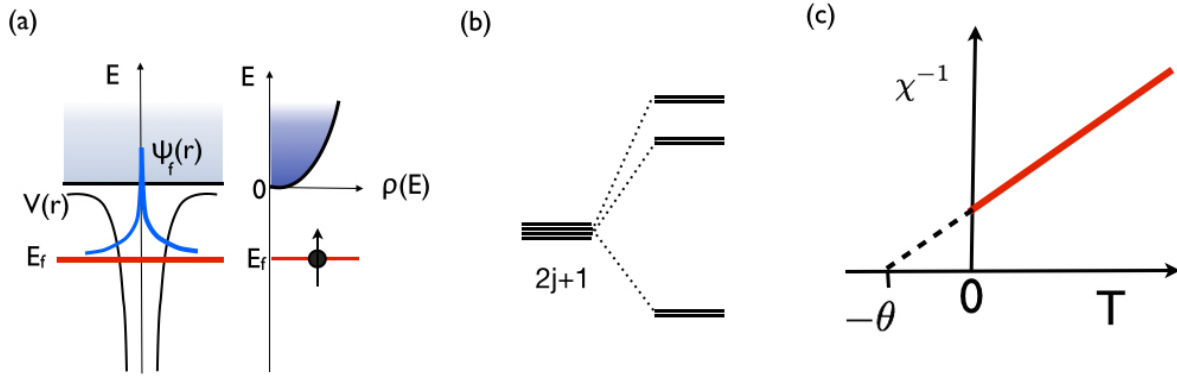


Fig. 2: *a) In isolation, the localized states of an atom form a stable, sharp excitation lying below the continuum. (b) In a crystal, the $2j + 1$ -fold degenerate state splits into multiplets, typically forming a low-lying Kramers doublet. (c) The inverse of the Curie-Weiss susceptibility of local moments χ^{-1} is a linear function of temperature, intersecting zero at $T = -\theta$.*

The presence of such local moments inside a metal profoundly alters its properties. The physics of an isolated magnetic ion is described by the *Kondo model*

$$H = \sum_{k\sigma} \varepsilon_k c_{k\sigma}^\dagger c_{k\sigma} + \overbrace{J \psi^\dagger(0) \vec{\sigma} \psi(0) \cdot \vec{S}_f}^{\Delta H}, \quad (3)$$

where $c_{k\sigma}^\dagger$ creates a conduction electron of energy ε_k and momentum k , and $\psi^\dagger(0) = \mathcal{N}_s^{-1/2} \sum_k c_{k\sigma}^\dagger$ creates a conduction electron at the origin, where \mathcal{N}_s is the number of sites in the lattice. The conduction sea interacts with the local moment via an antiferromagnetic contact interaction of strength J . The antiferromagnetic sign ($J > 0$) of this interaction is an example of *superexchange*, first predicted by Philip W. Anderson [4, 5], which results from high-energy valence fluctuations. Jun Kondo [6] first analyzed the effect of this scattering, showing that, as the temperature is lowered, the effective strength of the interaction grows logarithmically, according to

$$J \rightarrow J(T) = J + 2J^2 \rho \ln \frac{D}{T} \quad (4)$$

where ρ is the density of states of the conduction sea (per spin) and D is the band width. The growth of this interaction enabled Kondo to understand why in many metals at low temperatures the resistance starts to rise as the temperature is lowered, giving rise to a *resistance minimum*. Today, we understand this logarithmic correction as a renormalization of the Kondo coupling constant, resulting from the fact that, as the temperature is lowered, more and more high-frequency quantum spin fluctuations become coherent, and these strengthen the Kondo interaction. The effect is closely analogous to the growth of the strong interaction between quarks, and like quarks, the local moment in the Kondo effect is *asymptotically free* at high energies. However, as you can see from the above equation, once the temperature becomes of the order

$$T_K \sim D \exp \left[-\frac{1}{2J\rho} \right]$$

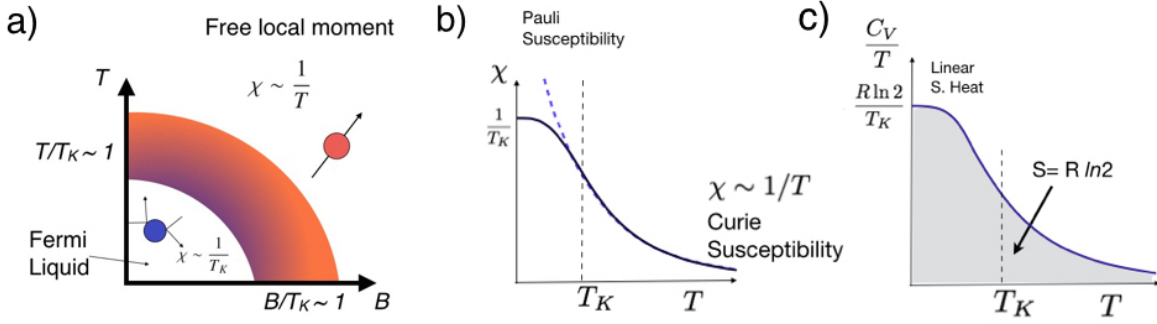


Fig. 3: (a) Schematic temperature-field phase diagram of the Kondo effect. At fields and temperatures large compared with the Kondo temperature T_K , the local moment is unscreened with a Curie susceptibility. At temperatures and fields small compared with T_K , the local moment is screened, forming an elastic scattering center within a Landau-Fermi liquid with a Pauli susceptibility $\chi \sim \frac{1}{T_K}$. (b) Schematic susceptibility curve for the Kondo effect, showing the cross-over from Curie susceptibility at high temperatures to Pauli susceptibility at temperatures below the Kondo temperature T_K . (c) Specific heat curve for the Kondo effect. Since the total area is the full spin entropy $R \ln 2$ and the width is of order T_K , the height must be of order $\gamma \sim R \ln 2 / T_K$. This sets the scale for the zero-temperature specific heat coefficient.

the correction becomes as large as the original perturbation, and at lower temperatures, the Kondo interaction can no longer be treated perturbatively. In fact, non-perturbative methods tell us that this interaction scales to strong coupling at low energies, causing electrons in the conduction sea to magnetically screen the local moment to form an inert *Kondo singlet* denoted by

$$|GS\rangle = \frac{1}{\sqrt{2}} \left(|\uparrow\downarrow\rangle - |\downarrow\uparrow\rangle \right), \quad (5)$$

where the thick arrow refers to the spin state of the local moment and the thin arrow refers to the spin state of a bound electron at the site of the local moment. The key features of the impurity Kondo effect are

- The electron fluid surrounding the Kondo singlet forms a Fermi liquid, with a Pauli susceptibility $\chi \sim 1/T_K$.
- The local moment is a kind of qubit that entangles with the conduction sea to form a singlet. As the temperature T is raised, the entanglement entropy converts to thermal entropy, given by the integral of the specific heat coefficient,

$$S(T) = \int_0^T dT' \frac{C_V(T')}{T'}.$$

Since the total area under the curve, $S(T \rightarrow \infty) = R \ln 2$ per mole, is the high-temperature spin entropy, and since the characteristic width is the Kondo temperature, it follows that the characteristic zero-temperature specific heat coefficient must be of the order of the inverse Kondo temperature: $\gamma = \frac{C_V}{T}(T \rightarrow 0) \sim R \ln 2 / T_K$ (see Fig. 3b).

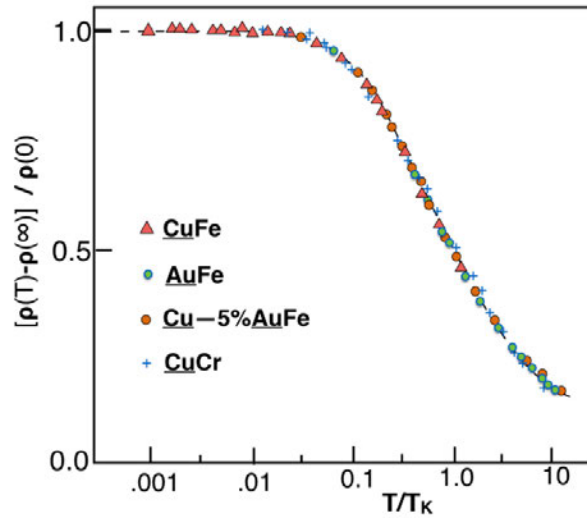


Fig. 4: Temperature dependence of resistivity associated with scattering from an impurity spin from [7, 8]. The resistivity saturates at the unitarity limit at low temperatures, due to the formation of the Kondo resonance. Adapted from [7].

- The only scale in the physics is T_K . For example, the resistivity created by magnetic scattering off the impurity has a universal temperature dependence

$$\frac{R(T)}{R_U} = n_i \Phi\left(\frac{T}{T_K}\right) \quad (6)$$

where n_i is the concentration of magnetic impurities, $\Phi(x)$ is a universal function and ρ_U is the unit of *unitary resistance* (basically resistance with a scattering rate of order the Fermi energy)

$$R_U = \frac{2ne^2}{\pi m\rho}. \quad (7)$$

Experiment confirms that the resistivity in the Kondo effect can indeed be scaled onto a single curve that fits forms derived from the Kondo model (see Fig 4).

- The scattering off the Kondo singlet is resonantly confined to a narrow region of order T_K , called the *Kondo* or *Abrikosov-Suhl* resonance.

1.3 The Kondo lattice

In a heavy-fermion material, containing a lattice of local moments, the Kondo effect develops *coherence*. In a single impurity, a Kondo singlet scatters electrons without conserving momentum, giving rise to a huge build-up of resistivity at low temperatures. However, in a lattice with translational symmetry, this same elastic scattering now conserves momentum, and this leads to coherent scattering off the Kondo singlets. In the simplest heavy-fermion metals, this leads to a dramatic reduction in the resistivity at temperatures below the Kondo temperature.

As a simple example, consider CeCu_6 a classic heavy-fermion metal. Naively, CeCu_6 is just a copper alloy in which 14% of the copper atoms are replaced by cerium, yet this modest replacement radically alters the metal. In this material, it actually proves possible to follow the development of coherence from the dilute single-ion Kondo limit to the dense Kondo lattice by forming the alloy $\text{La}_{1-x}\text{Ce}_x\text{Cu}_6$. Lanthanum is isoelectronic to cerium but has an empty f shell, so the limit $x \rightarrow 0$ corresponds to the dilute Kondo limit, and in this limit the resistivity follows the classic Kondo curve. However, as the concentration of cerium increases, the resistivity curve starts to develop a coherence maximum and in the concentrated limit drops to zero with the characteristic T^2 dependence of a Landau-Fermi liquid (see Fig. 6).

CeCu_6 displays the following classic features of a heavy-fermion metal:

- A Curie-Weiss susceptibility $\chi \sim (T + \theta)^{-1}$ at high temperatures.
- A paramagnetic spin susceptibility $\chi \sim \text{const.}$ at low temperatures.
- A dramatically enhanced linear specific heat $C_V = \gamma T$ at low temperatures, where in CeCu_6 $\gamma \sim 1000 \text{ mJ/mol/K}^2$ is about 1000 times larger than in copper.
- A quadratic temperature dependence of the low-temperature resistivity $\rho = \rho_o + AT^2$.

In a Landau-Fermi liquid, the magnetic susceptibility χ and the linear specific heat coefficient $\gamma = C_V/T|_{T \rightarrow 0}$ are given by

$$\chi = (\mu_B)^2 \frac{N^*(0)}{1 + F_0^a} \quad (8)$$

$$\gamma = \frac{\pi^2 k_B^2}{3} N^*(0) \quad (9)$$

where $N^*(0) = \frac{m^*}{m} N(0)$ is the renormalized density of states, and F_0^a is the spin-dependent part of the s -wave interaction between quasiparticles. One of the consequences of Fermi-liquid theory is that the density of states factors out of the Sommerfeld or Wilson ratio between the susceptibility and linear specific heat coefficient,

$$W = \frac{\chi}{\gamma} = \left(\frac{\mu_B}{2\pi k_B} \right)^2 \frac{1}{1 + F_0^a}. \quad (10)$$

In heavy-fermion metals, this ratio remains approximately fixed across several decades of variation in χ and γ . This allows us to understand heavy-fermion metals as a lattice version of the Kondo effect that gives rise to a renormalized density of states $N^*(0) \sim 1/T_K$.

The discovery of heavy-electron compounds in the 1970s led Mott [9] and Doniach [10] to propose that heavy-electron systems should be modeled as a *Kondo lattice*, where a dense array of local moments interacts with the conduction sea via an antiferromagnetic interaction J . In such a lattice, the local moments polarize the conduction sea, and the resulting Friedel oscillations in the magnetization give rise to an antiferromagnetic RKKY (Ruderman Kittel Kasuya Yosida) magnetic interaction [11–13] that tends to order the local moments. Mott and Doniach realized that this interaction must compete with the Kondo effect.

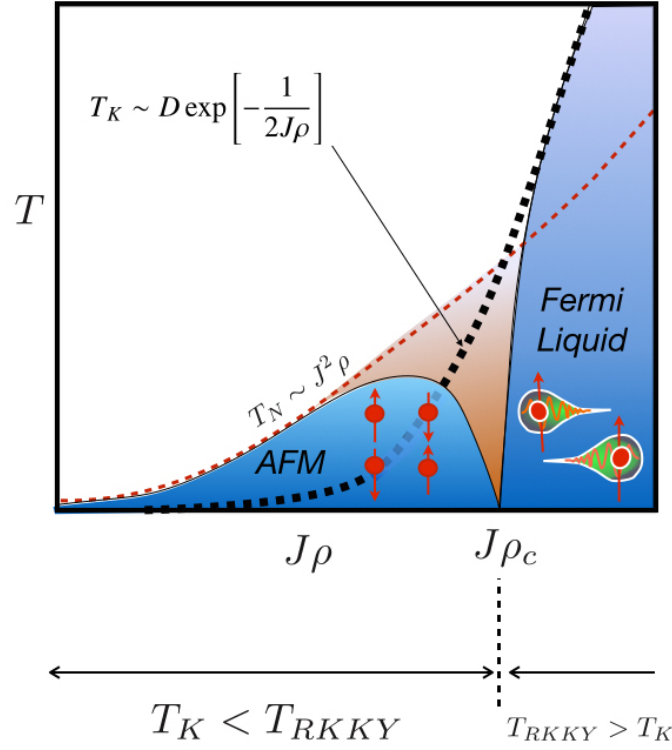


Fig. 5: Doniach phase diagram for the Kondo lattice, illustrating the antiferromagnetic regime and the heavy-fermion regime for $T_K < T_{\text{RKKY}}$ and $T_K > T_{\text{RKKY}}$ respectively. The effective Fermi temperature of the heavy Fermi liquid is indicated as a solid line. Experimental evidence suggests that in many heavy-fermion materials this scale drops to zero at the antiferromagnetic quantum critical point.

The simplest Kondo lattice Hamiltonian [14] is

$$H = \sum_{\mathbf{k}\sigma} \varepsilon_{\mathbf{k}} c_{\mathbf{k}\sigma}^\dagger c_{\mathbf{k}\sigma} + J \sum_j \vec{S}_j \cdot c_{j\alpha}^\dagger \vec{\sigma}_{\alpha\beta} c_{j\beta}, \quad (11)$$

where

$$c_{j\alpha}^\dagger = \frac{1}{\sqrt{\mathcal{N}_s}} \sum_{\mathbf{k}} c_{\mathbf{k}\alpha}^\dagger e^{-i\mathbf{k}\cdot\mathbf{R}_j} \quad (12)$$

creates an electron at site j . Mott and Doniach [9, 10] pointed out that there are two energy scales in the Kondo lattice: the Kondo temperature $T_K \sim D e^{-1/(2J\rho)}$ and the RKKY scale $E_{\text{RKKY}} = J^2 \rho$.

For small $J\rho$, $E_{\text{RKKY}} \gg T_K$ leading to an antiferromagnetic ground state, but when $J\rho$ is large, $T_K \gg E_{\text{RKKY}}$, stabilizing a ground state in which every site in the lattice resonantly scatters electrons. Based on a simplified one-dimensional *Kondo necklace* model [15], Doniach conjectured [10] that the transition between the antiferromagnet and the dense Kondo ground state is a continuous quantum phase transition. Experiment confirms this conjecture, and today we have several examples of such quantum critical points, including CeCu_6 doped with gold to form $\text{CeCu}_{6-x}\text{Au}_x$ and CeRhIn_5 under pressure [16–18]. In the fully developed Kondo lattice, the ground state Bloch's theorem ensures that the resonant elastic scattering at each site will

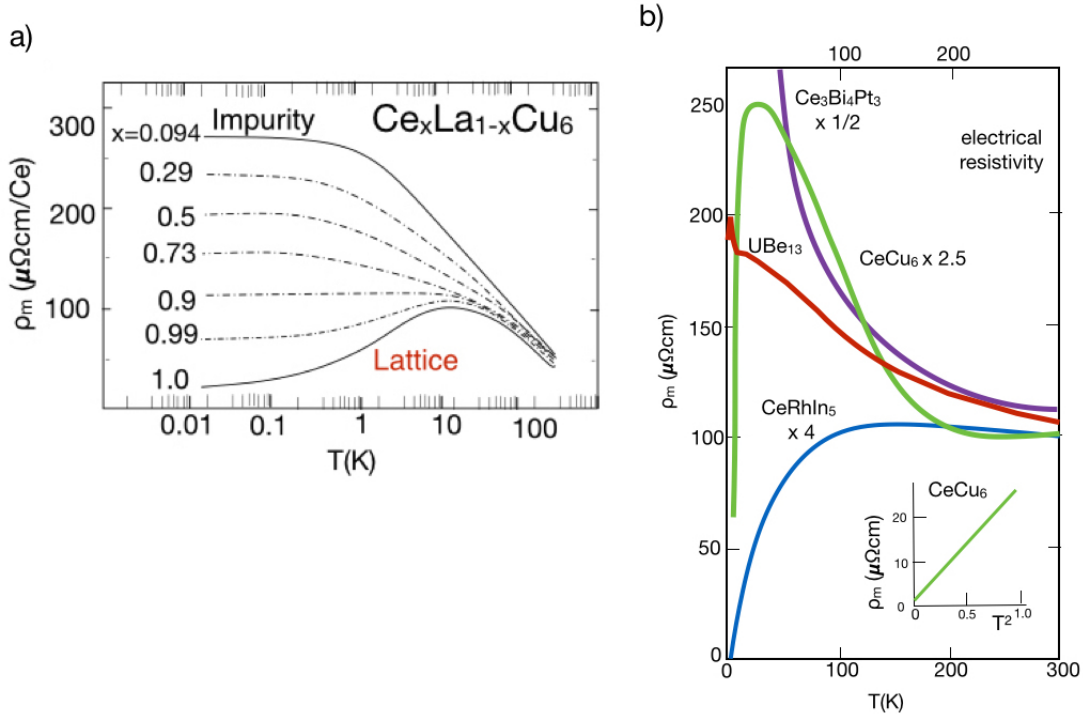


Fig. 6: (a) Resistivity of $\text{Ce}_x\text{La}_{1-x}\text{Cu}_6$. Dilute Ce atoms in LaCu_6 exhibit a classic Kondo resistivity, but as the Ce concentration becomes dense, elastic scattering off each Ce atom leads to the development of a coherent heavy-fermion metal. (b) Resistivities of four heavy-fermion materials showing the development of coherence. A variety of antiferromagnetic, Fermi liquid, superconducting and insulating states are formed (see text).

generate a renormalized f band of width $\sim T_K$. In contrast with the impurity Kondo effect, here elastic scattering at each site acts coherently. For this reason, as the heavy-electron metal develops at low temperatures, its resistivity drops towards zero (see Fig. 6b).

In a Kondo lattice, spin entanglement is occurring on a truly macroscopic scale, but this entanglement need not necessarily lead to a Fermi liquid. Experimentally, many other possibilities are possible. Here are some examples:

- $\text{Ce}_3\text{Bi}_4\text{Pt}_3$, a Kondo insulator in which the formation of Kondo singlets with the Ce moments drives the development of a small insulating gap at low temperatures.
- CeRhIn_5 , an antiferromagnet on the brink of forming a Kondo lattice, which under pressure becomes a heavy-fermion superconductor with $T_c = 2$ K.
- UBe_{13} a heavy-fermion superconductor that transitions directly from an incoherent metal with resistivity $200 \mu\Omega\text{cm}$ into a superconducting state.

Each of these materials has qualitatively the same high-temperature Curie-Weiss magnetism and the same Kondo resistivity at high temperatures due to incoherent scattering off the local moments. However at low temperatures, the scattering off the magnetic Ce ions becomes coherent and new properties develop.

2 Kondo insulators: the simplest heavy fermions

In many ways, the Kondo insulator is the simplest ground state of the Kondo lattice. The first Kondo insulator (KI) SmB_6 was discovered almost fifty years ago [19], and today there are several known examples, including $\text{Ce}_3\text{Bi}_4\text{Pt}_3$. At room temperature, these KIs are metals containing a dense array of magnetic moments, yet on cooling they develop a narrow gap due the formation of *Kondo singlets* that screen the local moments [20–23]. We can gain a lot of insight by examining the strong-coupling limit, in which the dispersion of the conduction sea is much smaller than the Kondo coupling J . Consider a simple tight-binding Kondo lattice

$$H = -t \sum_{(i,j)\sigma} (c_{i\sigma}^\dagger c_{j\sigma} + \text{H.c.}) + J \sum_{j,\alpha\beta} \vec{\sigma}_j \cdot \vec{S}_j, \quad \vec{\sigma}_j \equiv (c_{j\beta}^\dagger \vec{\sigma}_{\beta\alpha} c_{j\alpha}) \quad (13)$$

in which $t/J \ll 1$ is a small parameter. In this limit, the inter-site hopping is a perturbation to the on-site Kondo interaction,

$$H \xrightarrow{t/J \rightarrow 0} J \sum_{j,\alpha\beta} \vec{\sigma}_j \cdot \vec{S}_j + \mathcal{O}(t), \quad (14)$$

and the corresponding ground state shows the formation of a spin singlet at each site, denoted by the wavefunction

$$|KI\rangle = \prod_j \frac{1}{\sqrt{2}} \left(\uparrow_j \downarrow_j - \downarrow_j \uparrow_j \right) \quad (15)$$

where the double and single arrows denote the localized moment and conduction electron respectively.

Each singlet has a ground-state energy $E = -3J/2$ per site and a singlet-triplet spin gap of magnitude $\Delta E = 2J$. Moreover, if we remove an electron from site i , we break a Kondo singlet and create an unpaired spin with excited energy $3J/2$,

$$|\text{qp}^+, i \uparrow\rangle = \uparrow_i \prod_{j \neq i} \frac{1}{\sqrt{2}} \left(\uparrow_j \downarrow_j - \downarrow_j \uparrow_j \right) = \sqrt{2} c_{i\downarrow} |KI\rangle, \quad (16)$$

as illustrated in Fig 7(a). Similarly, if we add an electron, we create an electron quasiparticle, corresponding to an unpaired local moment and a doubly occupied conduction electron orbital

$$|\text{qp}^-, i \uparrow\rangle = \uparrow_i \left(\uparrow_i \downarrow_i \right) \prod_{j \neq i} \frac{1}{\sqrt{2}} \left(\uparrow_j \downarrow_j - \downarrow_j \uparrow_j \right) = \sqrt{2} c_{j\uparrow}^\dagger |KI\rangle, \quad (17)$$

as illustrated in Fig 7b.

If we now reintroduce the hopping $-t$ between sites, then these quasiparticle excitations become mobile, as illustrated in Fig. 7 a and b. From the explicit form of the states, we find that the nearest-neighbor hopping matrix elements are $\langle \text{qp}^\pm, i\sigma | H | \text{qp}^\pm, j\sigma \rangle = \pm t/2$, giving quasiparticle energies

$$E_{\text{qp}^\pm}(\mathbf{k}) = \pm t(c_x + c_y + c_z) + \frac{3}{2}J. \quad (18)$$

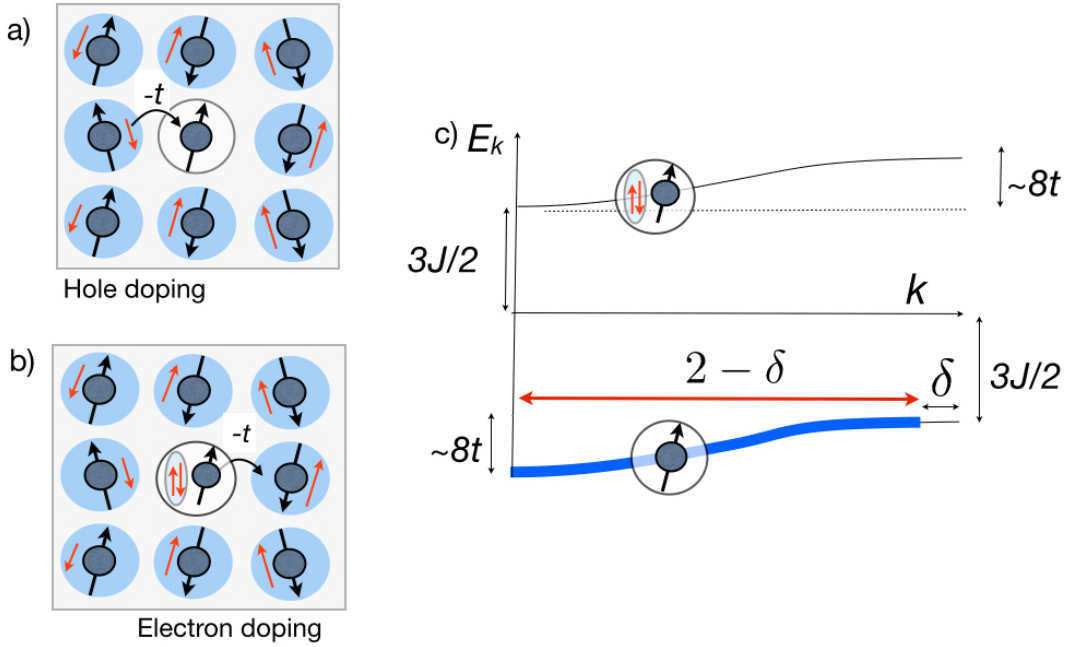


Fig. 7: Showing (a) hole and (b) electron doping of a strong-coupling Kondo insulator. (c) Dispersion of strong-coupling Kondo insulator. A small amount of hole doping δ gives rise to a large Fermi surface containing $2 - \delta$ heavy electrons.

To transform from the quasiparticle to the electron basis, we need to reverse the sign of the hole (qp^+) dispersion to obtain the valence band dispersion, so that the band energies predicted by the strong-coupling limit of the Kondo lattice are

$$E_{\mathbf{k}}^{\pm} = -t(c_x + c_y + c_z) \pm \frac{3}{2}J, \quad (19)$$

separated by an energy $3J$ as shown in Fig. 7c. Note that these are *hard core* fermions that cannot occupy the same lattice site simultaneously.

In this way, the half-filled strong coupling Kondo lattice forms an insulator with a charge gap of size $3J$ and a spin gap of size $2J$. Notice finally that if we dope the insulator with an amount δ of holes, we form a band of heavy fermions. In this way, Kondo insulators can be considered the parent states of heavy-electron materials. However, we would like to examine the physics of a Kondo lattice at weak coupling, and to do this requires a different approach.

3 Large- N expansion for the Kondo Lattice

3.1 Philosophy and formulation

One of the great difficulties with the Kondo lattice is that there is no natural small parameter to carry out an approximate treatment. One way around this difficulty is to use a large- N expansion, in which we extend the number of spin components of the electrons from 2 to N . Historically, Anderson [24] pointed out that the large spin-orbit coupling in heavy-fermion compounds generates (if we ignore crystal fields) a large spin degeneracy $N = 2j + 1$, furnishing a small

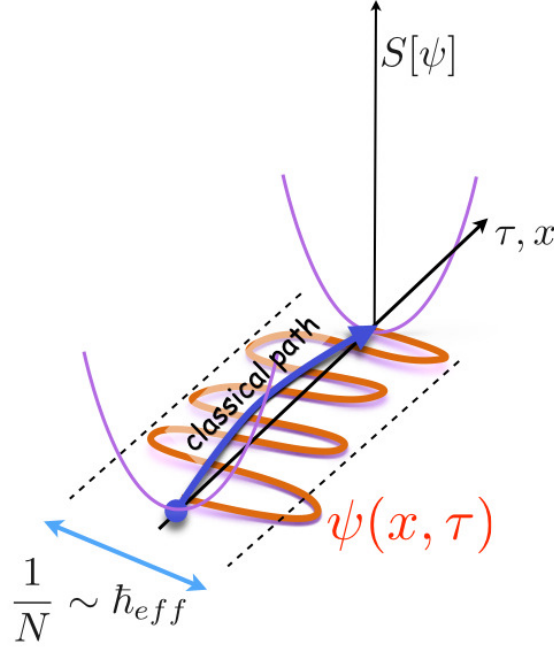


Fig. 8: Illustration of the convergence of a quantum path integral about a semi-classical trajectory in the large- N limit.

parameter $1/N$ for a controlled expansion about the limit $N \rightarrow \infty$. One of the observations arising from Anderson’s idea [25, 26] is that the RKKY interaction becomes negligible (of order $\mathcal{O}(1/N^2)$) in this limit, and the Kondo lattice ground state becomes stable. This observation opened the way to path-integral mean-field treatments of the Kondo lattice [26–31].

The basic idea of the large- N limit is to examine a limit where every term in the Hamiltonian grows extensively with N . In the path integral for the partition function, the corresponding action then grows extensively with N , so that

$$Z = \int \mathcal{D}[\psi] e^{-NS} = \int \mathcal{D}\psi \exp \left[-\frac{S}{1/N} \right] \equiv \int \mathcal{D}[\psi] \exp \left[-\frac{S}{\hbar_{\text{eff}}} \right]. \quad (20)$$

Here $1/N \sim \hbar_{\text{eff}}$ behaves as an effective Planck constant for the theory, focusing the path integral into a non-trivial “semi-classical” or “mean-field” solution as $\hbar_{\text{eff}} \rightarrow 0$. As $N \rightarrow \infty$, the quantum fluctuations of intensive variables \hat{a} , such as the electron density per spin, become smaller and smaller, scaling as $\langle \delta a^2 \rangle / \langle a^2 \rangle \sim 1/N$, causing the path integral to focus around a non-trivial mean-field trajectory. In this way, one can obtain new results by expanding around the solvable large- N limit in powers of $1/N$ (Fig. 8).

We will use a simplified Kondo lattice model introduced by Read and Newns [26], in which all electrons have a spin degeneracy $N = 2j + 1$,

$$H = \sum_{\mathbf{k}\alpha} \varepsilon_{\mathbf{k}} c_{\mathbf{k}\alpha}^\dagger c_{\mathbf{k}\alpha} + \frac{J}{N} \sum_{j,\alpha\beta} c_{j\beta}^\dagger c_{j\alpha} S_{\alpha\beta}(j). \quad (21)$$

where $c_{j\alpha}^\dagger = \frac{1}{\sqrt{N_s}} \sum_{\mathbf{k}} c_{\mathbf{k}\alpha}^\dagger e^{-i\mathbf{k}\cdot\mathbf{R}_j}$ creates an electron localized at site j , and the spin of the local moment at position \mathbf{R}_j is represented by pseudo-fermions

$$S_{\alpha\beta}(j) = f_{j\alpha}^\dagger f_{j\beta} - \frac{n_f(j)}{N} \delta_{\alpha\beta}. \quad (22)$$

This representation requires that we set a value for the conserved f occupancy $n_f(j) = Q$ at each site. This interaction can be rewritten in a factorized form

$$H = \sum_{\mathbf{k}\alpha} \varepsilon_{\mathbf{k}} c_{\mathbf{k}\alpha}^\dagger c_{\mathbf{k}\alpha} - \frac{J}{N} \sum_{j,\alpha\beta} : (c_{j\beta}^\dagger f_{j\beta}) (f_{j\alpha}^\dagger c_{j\alpha}) : \quad (23)$$

Read-Newns model for the Kondo lattice

where the potential scattering terms resulting from the rearrangement of the f -operators have been absorbed into a shift of the chemical potential. Note that

- the model has a global $SU(N)$ symmetry associated with the conserved magnetization.
- the Read-Newns (RN) model is a lattice version of the Coqblin-Schrieffer Hamiltonian [32] introduced to describe the Kondo interaction in strongly spin-orbit coupled rare-earth ions. While the Coqblin-Schrieffer interaction is correct at each site, the assumption that the $SU(N)$ spin is conserved by electron hopping is an oversimplification. (This is a price one pays for a solvable model.)
- in this factorized form, the antiferromagnetic Kondo interaction is attractive.
- the coupling constant has been scaled to vary as J/N to ensure that the interaction grows extensively with N . The interaction involves a product of two terms that scale as $O(N)$, so that $J/N \times O(N^2) \sim O(N)$.
- the RN model also has a **local gauge invariance**: The absence of f charge fluctuations allows us to change the phase of the f -electrons *independently* at each site

$$f_{j\sigma} \rightarrow e^{i\phi_j} f_{j\sigma}. \quad (24)$$

A tricky issue concerns the value we give to the conserved charge $n_f = Q$. In the physical models of interest, $n_f = 1$ at each site, so one might be inclined to explicitly maintain this condition. However, the large- N expansion requires that the action is extensive in N , and this forces us to consider more general classes of solutions where Q scales with N so that the filling factor $q = Q/N$ is finite as $N \rightarrow \infty$. Thus if we are interested in a Kramers-doublet Kondo model, we take the half-filled case $q = 1/2$, $Q = N/2$, but if we want to understand a $j = 7/2$ Yb^{3+} atom without crystal fields, then in the physical system $N = 2j + 1 = 8$, and we should fix $q = Q/N = 1/8$.

The partition function for the Kondo lattice is then

$$Z = \text{Tr} \left[e^{-\beta H} \prod_j \delta(\hat{n}_f(j) - Q) \right] \quad (25)$$

where $\delta(\hat{n}_f(j) - Q)$ projects out the states with $n_f(j) = Q$ at site j . By re-writing the delta function as a Fourier transform, the partition function can be rewritten as a path-integral,

$$Z = \int \mathcal{D}[\psi^\dagger, \psi, \lambda] \exp \left[- \int_0^\beta d\tau \overbrace{(\psi^\dagger \partial_\tau \psi + H[\bar{\psi}, \psi, \lambda])}^{L[\psi^\dagger, \psi, \lambda]} \right] \quad (26)$$

where $\psi^\dagger \equiv (\{c^\dagger\}, \{f^\dagger\})$ schematically represent the conduction and f -electron fields,

$$H[\lambda] = \sum_{\mathbf{k}\alpha} \varepsilon_{\mathbf{k}} c_{\mathbf{k}\alpha}^\dagger c_{\mathbf{k}\alpha} - \frac{J}{N} \sum_{j,\alpha\beta} : (c_{j\beta}^\dagger f_{j\beta}) (f_{j\alpha}^\dagger c_{j\alpha}) : + \sum_j \lambda_j (n_{fj} - Q). \quad (27)$$

The field λ_j is a fluctuating Lagrange multiplier that enforces the constraint $n_j = Q$ at each site. Next we carry out a Hubbard-Stratonovich transformation on the interaction,

$$- \frac{J}{N} \sum_{\alpha\beta} (c_{j\beta}^\dagger f_{j\beta}) (f_{j\alpha}^\dagger c_{j\alpha}) \rightarrow \sum_\alpha [\bar{V}_j (c_{j\alpha}^\dagger f_{j\alpha}) + (f_{j\alpha}^\dagger c_{j\alpha}) V_j] + N \frac{\bar{V}_j V_j}{J}. \quad (28)$$

In the original Kondo model, we started out with an interaction between electrons and spins. Now, by carrying out the Hubbard-Stratonovich transformation, we have formulated the interaction as the exchange of a charged boson

$$\text{Diagram (29)} \quad (29)$$

$$- \frac{J}{N} \sum_{\mathbf{k}, \mathbf{k}', \alpha, \beta} (c_{\beta}^\dagger f_{\beta}) (f_{\alpha}^\dagger c_{\alpha}) \quad (30)$$

where the solid lines represent the conduction electron propagators, and the dashed lines represent the f -electron operators. Notice how the bare amplitude associated with the exchange boson is frequency independent, i.e., the interaction is instantaneous. Physically, we may interpret this exchange process as due to an intermediate valence fluctuation.

The path integral now involves an additional integration over the hybridization fields V and \bar{V}

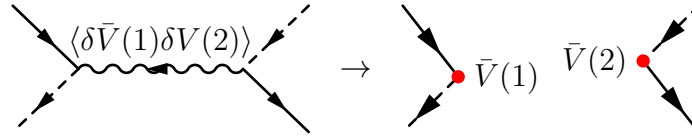
$$Z = \int \mathcal{D}[\bar{V}, V, \lambda] \int \mathcal{D}[\psi^\dagger, \psi] \exp \left[- \int_0^\beta (\psi^\dagger \partial_\tau \psi + H[\bar{V}, V, \lambda]) \right] \quad (31)$$

$$H[\bar{V}, V, \lambda] = \sum_{\mathbf{k}} \varepsilon_{\mathbf{k}} c_{\mathbf{k}\sigma}^\dagger c_{\mathbf{k}\sigma} + \sum_j \left[\bar{V}_j (c_{j\sigma}^\dagger f_{j\sigma}) + (f_{j\sigma}^\dagger c_{j\sigma}) V_j + \lambda_j (n_{fj} - Q) + N \frac{\bar{V}_j V_j}{J} \right]$$

Read-Newns path integral for the Kondo lattice

where we have suppressed summation signs for repeated spin indices (summation convention).

The RN path integral allows us to develop a mean-field description of the many-body Kondo scattering processes that captures the physics and is asymptotically exact as $N \rightarrow \infty$. In this approach, the condensation of the hybridization field describes the formation of bound states between spins and electrons that cannot be dealt with in perturbation theory. Bound states induce long-range temporal correlations in scattering: Once the hybridization condenses, the interaction lines break-up into independent anomalous scattering events, denoted by



The hybridization V in the RN action carries the local $U(1)$ gauge charge of the f -electrons, giving rise to an important local gauge invariance:

$$f_{j\sigma} \rightarrow e^{i\phi_j} f_{j\sigma}, \quad V_j \rightarrow e^{i\phi_j} V_j, \quad \lambda_j \rightarrow \lambda_j - i\dot{\phi}_j(\tau). \quad (32)$$

Read Newns gauge transformation

This invariance can be used to choose a gauge in which V_j is real by absorbing the phase of the hybridization $V_j = |V_j|e^{i\phi_j}$ into the f -electron. In the radial gauge,

$$Z = \int \mathcal{D}[|V|, \lambda] \int \mathcal{D}[\psi^\dagger, \psi] \exp \left[- \int_0^\beta \overbrace{(\psi^\dagger \partial_\tau \psi + H[|V|, \lambda])}^{S[|V|, \lambda, \psi^\dagger, \psi]} \right]$$

$$H[|V|, \lambda] = \sum_{\mathbf{k}} \varepsilon_{\mathbf{k}} c_{\mathbf{k}\sigma}^\dagger c_{\mathbf{k}\sigma} + \sum_j \left[|V_j| \left(c_{j\sigma}^\dagger f_{j\sigma} + f_{j\sigma}^\dagger c_{j\sigma} \right) + \lambda_j (n_{fj} - Q) + N \frac{|V_j|^2}{J} \right] \quad (33)$$

Read Newns path integral: radial gauge

Subsequently, when we use the radial gauge, we will drop the moduli signs. The interesting feature about this Hamiltonian is that with the real hybridization, the conduction and f electrons now transform under a single global $U(1)$ gauge transformation, i.e the f electrons have become *charged*.

3.2 Mean-field theory

The interior fermion integral in the path integral (33) defines an effective action $S_E[V, \lambda]$ by the relation

$$Z_E = \exp[-NS_E[V, \lambda]] \equiv \int \mathcal{D}[\psi^\dagger, \psi] \exp[-S[V, \lambda, \psi^\dagger, \psi]], \quad (34)$$

The extensive growth of the effective action with N means that at large N , the integration in (31) is dominated by its stationary points, allowing us to dispense with the integrals over V and λ .

$$Z = \int \mathcal{D}[\lambda, V] \exp[-NS_E[V, \lambda]] \approx \exp[-NS_E[V, \lambda]] \Big|_{\text{Saddle Point}} \quad (35)$$

In practice, we seek uniform, static solutions, $V_j(\tau) = V$, $\lambda_j(\tau) = \lambda$. In this case the saddle-point partition function $Z_E = \text{Tr}e^{-\beta H_{\text{MFT}}}$ is simply the partition function of the static mean-field Hamiltonian

$$\begin{aligned} H_{\text{MFT}} &= \sum_{\mathbf{k}\sigma} \left(c_{\mathbf{k}\sigma}^\dagger, f_{\mathbf{k}\sigma}^\dagger \right) \overbrace{\begin{pmatrix} \varepsilon_{\mathbf{k}} & V \\ \bar{V} & \lambda \end{pmatrix}}^{\underline{h}(\mathbf{k})} \begin{pmatrix} c_{\mathbf{k}\sigma} \\ f_{\mathbf{k}\sigma} \end{pmatrix} + N\mathcal{N}_s \left(\frac{|V|^2}{J} - \lambda q \right) \\ &= \sum_{\mathbf{k}\sigma} \psi_{\mathbf{k}\sigma}^\dagger \underline{h}(\mathbf{k}) \psi_{\mathbf{k}\sigma} + N\mathcal{N}_s \left(\frac{|V|^2}{J} - \lambda q \right). \end{aligned} \quad (36)$$

Here, $f_{\mathbf{k}\sigma}^\dagger = \frac{1}{\sqrt{N_s}} \sum_j f_{j\sigma}^\dagger e^{i\mathbf{k}\cdot\mathbf{R}_j}$ is the Fourier transform of the f -electron field and we have introduced the two-component notation

$$\psi_{\mathbf{k}\sigma} = \begin{pmatrix} c_{\mathbf{k}\sigma} \\ f_{\mathbf{k}\sigma} \end{pmatrix}, \quad \psi_{\mathbf{k}\sigma}^\dagger = \left(c_{\mathbf{k}\sigma}^\dagger, f_{\mathbf{k}\sigma}^\dagger \right), \quad \underline{h}(\mathbf{k}) = \begin{pmatrix} \varepsilon_{\mathbf{k}} & V \\ \bar{V} & \lambda \end{pmatrix}. \quad (37)$$

We should think about H_{MFT} as a renormalized Hamiltonian, describing the low-energy quasiparticles moving through a self-consistently determined array of resonant scattering centers. Later, we will see that the f -electron operators are composite objects, formed as bound states between spins and conduction electrons.

The mean-field Hamiltonian can be diagonalized in the form

$$H_{\text{MFT}} = \sum_{\mathbf{k}\sigma} \left(a_{\mathbf{k}\sigma}^\dagger, b_{\mathbf{k}\sigma}^\dagger \right) \begin{pmatrix} E_{\mathbf{k}^+} & 0 \\ 0 & E_{\mathbf{k}^-} \end{pmatrix} \begin{pmatrix} a_{\mathbf{k}\sigma} \\ b_{\mathbf{k}\sigma} \end{pmatrix} + N\mathcal{N}_s \left(\frac{\bar{V}V}{J} - \lambda q \right). \quad (38)$$

Here $a_{\mathbf{k}\sigma}^\dagger = u_{\mathbf{k}} c_{\mathbf{k}\sigma}^\dagger + v_{\mathbf{k}} f_{\mathbf{k}\sigma}^\dagger$ and $b_{\mathbf{k}\sigma}^\dagger = -v_{\mathbf{k}} c_{\mathbf{k}\sigma}^\dagger + u_{\mathbf{k}} f_{\mathbf{k}\sigma}^\dagger$ are linear combinations of $c_{\mathbf{k}\sigma}^\dagger$ and $f_{\mathbf{k}\sigma}^\dagger$ playing the role of quasiparticle operators with corresponding energy eigenvalues

$$\det \left[E_{\mathbf{k}^\pm} \mathbf{1} - \begin{pmatrix} \varepsilon_{\mathbf{k}} & V \\ \bar{V} & \lambda \end{pmatrix} \right] = (E_{\mathbf{k}^\pm} - \varepsilon_{\mathbf{k}})(E_{\mathbf{k}^\pm} - \lambda) - |V|^2 = 0, \quad (39)$$

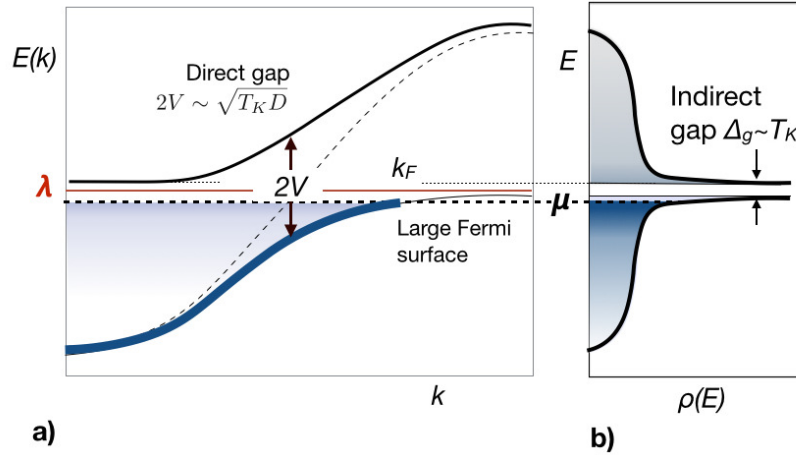


Fig. 9: (a) Dispersion for the Kondo lattice mean-field theory. (b) Renormalized density of states, showing a “hybridization gap” (Δ_g).

or

$$E_{\mathbf{k}\pm} = \frac{\varepsilon_{\mathbf{k}} + \lambda}{2} \pm \left[\left(\frac{\varepsilon_{\mathbf{k}} - \lambda}{2} \right)^2 + |V|^2 \right]^{\frac{1}{2}}, \quad (40)$$

and eigenvectors taking the BCS form

$$\begin{Bmatrix} u_{\mathbf{k}} \\ v_{\mathbf{k}} \end{Bmatrix} = \left[\frac{1}{2} \pm \frac{(\varepsilon_{\mathbf{k}} - \lambda)/2}{2\sqrt{\left(\frac{\varepsilon_{\mathbf{k}} - \lambda}{2}\right)^2 + |V|^2}} \right]^{\frac{1}{2}}. \quad (41)$$

The hybridized dispersion described by these energies is shown in Fig. 9.

Note that

- The Kondo effect injects an f band into the conduction sea, hybridizing with the conduction band to create two bands separated by a *direct* “hybridization gap” of size $2V$ and a much smaller *indirect* gap. If we put $\varepsilon_{\mathbf{k}} = \pm D$, we see that the upper and lower edges of the gap are given by

$$E^{\pm} = \frac{\mp D + \lambda}{2} \pm \sqrt{\left(\frac{\mp D - \lambda}{2} \right)^2 + V^2} \approx \lambda \pm \frac{V^2}{D}, \quad (D \gg \lambda) \quad (42)$$

so the indirect gap has a size $\Delta_g \sim 2V^2/D$, where D is the half bandwidth. We will see shortly that $V^2/D \sim T_K$ is basically the single-ion Kondo temperature, so that $V \sim \sqrt{T_K D}$ is the geometric mean of the bandwidth and Kondo temperature.

- In the case when the chemical potential lies in the gap, a *Kondo insulator* is formed.
- A conduction sea of electrons has been transformed into a heavy Fermi sea of holes.
- The Fermi surface volume *expands* in response to the formation of heavy electrons (see Fig. 10) to accommodate the total number of occupied quasiparticle states

$$N_{tot} = \left\langle \sum_{k\lambda\sigma} n_{k\lambda\sigma} \right\rangle = \langle \hat{n}_f + \hat{n}_c \rangle \quad (43)$$

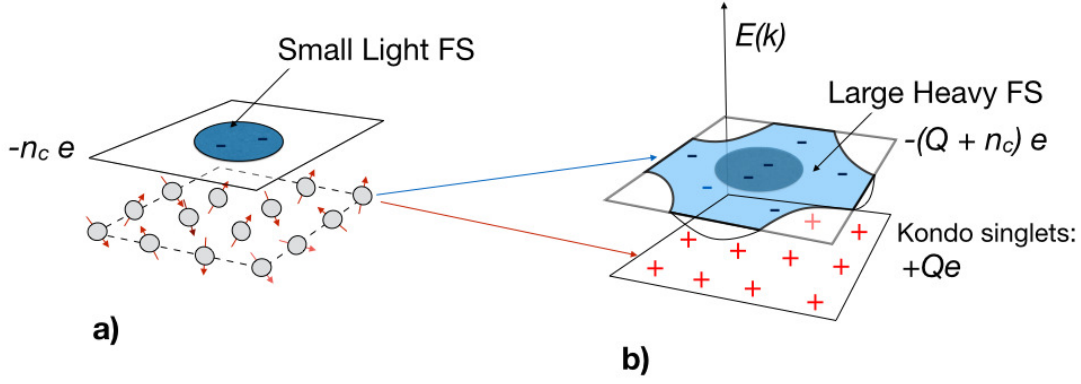


Fig. 10: (a) High-temperature state: small Fermi surface with a background of spins; (b) Low-temperature state: large Fermi surface develops against a background of positive charge. Each spin “ionizes” into Q heavy electrons, leaving behind a background of Kondo singlets, each with charge $+Qe$.

where $n_{k\lambda\sigma} = a_{k\lambda\sigma}^\dagger a_{k\lambda\sigma}$ is the number operator for the quasiparticles and n_c is the total number of conduction electrons. This means

$$N_{tot} = N \frac{V_{FS} a^3}{(2\pi)^3} = Q + n_c, \quad (44)$$

where a^3 is the volume of the unit cell. This is rather remarkable, for the expansion of the Fermi surface implies an increased *negative* charge density in the Fermi sea. Since charge is conserved, we are forced to conclude there is a compensating $+Q|e|$ charge density per unit cell provided by the Kondo singlets formed at each site, as illustrated in Fig. 10.

3.3 Free energy and saddle point

Let us now use the results of the last section to calculate the mean-field free energy F_{MFT} and determine self-consistently the parameters λ and V that set the scales of the Kondo lattice. By diagonalizing the mean-field Hamiltonian, we obtain

$$\frac{F}{N} = -T \sum_{\mathbf{k}, \pm} \ln \left[1 + e^{-\beta E_{\mathbf{k}\pm}} \right] + \mathcal{N}_s \left(\frac{V^2}{J} - \lambda q \right). \quad (45)$$

Let us discuss the ground state, in which only the lower band contributes to the free energy. As $T \rightarrow 0$, we can replace $-T \ln(1 + e^{-\beta E_{\mathbf{k}}}) \rightarrow \theta(-E_{\mathbf{k}}) E_{\mathbf{k}}$, so the ground-state energy $E_0 = F(T=0)$ involves an integral over the occupied states of the lower band:

$$\frac{E_o}{N\mathcal{N}_s} = \int_{-\infty}^0 dE \rho^*(E) E + \left(\frac{V^2}{J} - \lambda q \right), \quad (46)$$

where we have introduced the density of heavy-electron states $\rho^*(E) = \sum_{\mathbf{k}, \pm} \delta(E - E_{\mathbf{k}}^{(\pm)})$. Now by (39) the relationship between the energy E of the heavy electrons and the energy ε of the conduction electrons is

$$E = \varepsilon + \frac{V^2}{E - \lambda}.$$

As we sum over momenta \mathbf{k} within a given energy shell, there is a one-to-one correspondence between each conduction electron state and each quasiparticle state, so we can write $\rho^*(E)dE = \rho(\varepsilon)d\varepsilon$, where the density of heavy electron states

$$\rho^*(E) = \rho \frac{d\varepsilon}{dE} = \rho \left(1 + \frac{V^2}{(E - \lambda)^2} \right). \quad (47)$$

Here we have approximated the underlying conduction electron density of states by a constant $\rho = 1/(2D)$. The originally flat conduction electron density of states is now replaced by a hybridization gap, flanked by two sharp peaks of width approximately $\pi\rho V^2 \sim T_K$ (Fig. 9). Note that the lower bandwidth is lowered by an amount $-V^2/D$. With this information, we can carry out the integral over the energies to obtain

$$\frac{E_o}{N\mathcal{N}_s} = \rho \int_{-D-V^2/D}^0 dE E \left(1 + \frac{V^2}{(E - \lambda)^2} \right) + \left(\frac{V^2}{J} - \lambda q \right), \quad (48)$$

where we have assumed that the upper band is empty and that the lower band is partially filled. Carrying out the integral we obtain

$$\frac{E_o}{N\mathcal{N}_s} = -\frac{\rho}{2} \left(D + \frac{V^2}{D} \right)^2 + \frac{\Delta}{\pi} \int_{-D}^0 dE \left(\frac{1}{E - \lambda} + \frac{\lambda}{(E - \lambda)^2} \right) + \left(\frac{V^2}{J} - \lambda q \right) \quad (49)$$

$$= -\frac{D^2\rho}{2} + \frac{\Delta}{\pi} \ln \left(\frac{\lambda}{D} \right) + \left(\frac{V^2}{J} - \lambda q \right) \quad (50)$$

where we have replaced $\Delta = \pi\rho V^2$, which is the width of an isolated f -resonance, and have dropped terms of order $\mathcal{O}(\Delta^2/D)$. We can rearrange this expression, absorbing the bandwidth D and the Kondo coupling constant into a single Kondo temperature $T_K = De^{-1/J\rho}$ as follows

$$\frac{E_o}{N\mathcal{N}_s} = -\frac{D^2\rho}{2} + \frac{\Delta}{\pi} \ln \left(\frac{\lambda}{D} \right) + \left(\frac{\pi\rho V^2}{\pi\rho J} - \lambda q \right) \quad (51)$$

$$= -\frac{D^2\rho}{2} + \frac{\Delta}{\pi} \ln \left(\frac{\lambda}{D} \right) + \left(\frac{\Delta}{\pi\rho J} - \lambda q \right) \quad (52)$$

$$= -\frac{D^2\rho}{2} + \frac{\Delta}{\pi} \ln \left(\frac{\lambda}{De^{-\frac{1}{J\rho}}} \right) - \lambda q \quad (53)$$

$$= -\frac{D^2\rho}{2} + \frac{\Delta}{\pi} \ln \left(\frac{\lambda}{T_K} \right) - \lambda q. \quad (54)$$

This describes the energy of a family of Kondo lattice models with different $J(D)$ and cutoff D but fixed Kondo temperature. If we impose the constraint $\frac{\partial E_o}{\partial \lambda} = \langle n_f \rangle - Q = 0$ we obtain $\frac{\Delta}{\pi\lambda} - q = 0$, so

$$\frac{E_o(V)}{N\mathcal{N}_s} = \frac{\Delta}{\pi} \ln \left(\frac{\Delta}{\pi q e T_K} \right) - \frac{D^2\rho}{2}, \quad (\Delta = \pi\rho|V|^2) \quad (55)$$

Let us pause for a moment to consider this energy functional qualitatively. There are two points to be made:

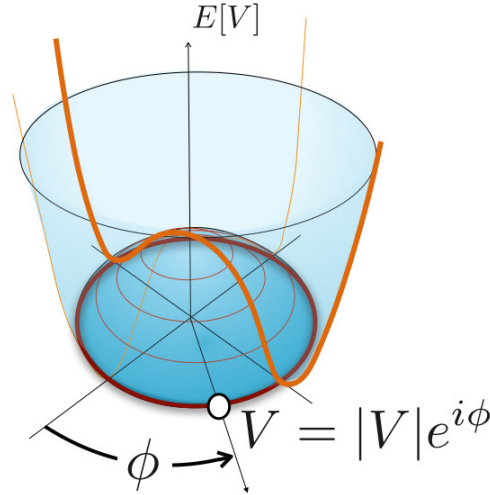


Fig. 11: Mexican hat potential for the Kondo Lattice, evaluated at constant $\langle n_f \rangle = Q$ as a function of a complex hybridization $V = |V|e^{i\phi}$

- The energy surface $E_0(V)$ is actually independent of the phase of $V = |V|e^{i\phi}$ (see Fig. 11), and has the form of Mexican hat at low temperatures. The minimum of this functional will then determine a family of saddle-point values $V = |V_0|e^{i\phi}$, where ϕ can have any value. If we differentiate the ground-state energy with respect to Δ , we obtain

$$0 = \frac{1}{\pi} \ln \left(\frac{\Delta}{\pi q T_K} \right)$$

or

$$\Delta = \pi q T_K$$

confirming that $\Delta \sim T_K$.

- The mean-field value of the constraint field λ is determined relative to the Fermi energy μ . Were we to introduce a slowly varying external potential field to the conduction electron sea, then the chemical potential would become locally shifted so that $\mu \rightarrow \mu + e\phi(t)$. So long as the field $\phi(t)$ is varied at a rate slowly compared with the Kondo temperature, the constraint field will always track with the chemical potential, and since the constraint field is pinned to the chemical potential, $\lambda \rightarrow \lambda + e\phi(t)$. In the process, the constraint term will become

$$\lambda(\hat{n}_f(j) - Q) \rightarrow \lambda(\hat{n}_f(j) - Q) + e\phi(t)(\hat{n}_f(j) - Q). \quad (56)$$

Since the f -electrons now couple to the external potential $e\phi$ we have to ascribe a physical charge $e = -|e|$ to them. By contrast, the $-Q$ term in the constraint must be interpreted as a “background positive charge” $|e|Q \equiv |e|$ per site. These lines of reasoning indicate that we should think of the Kondo effect as a *many-body ionization phenomenon* in which the neutral local moment splits up into a negatively charged heavy electron and a stationary positive background charge we can associate with the formation of a Kondo singlet.

3.4 The composite nature of the f -electron

The matrix Green's function of the Kondo lattice reminds us of the Nambu Green's function in superconductivity. It is given by

$$\mathcal{G}_{\mathbf{k}}(\tau) = -\langle \psi_{\mathbf{k}\sigma}(\tau) \psi_{\mathbf{k}\sigma}^\dagger(0) \rangle \equiv \begin{bmatrix} G_c(\mathbf{k}, \tau) & G_{cf}(\mathbf{k}, \tau) \\ G_{fc}(\mathbf{k}, \tau) & G_f(\mathbf{k}, \tau) \end{bmatrix} \quad (57)$$

where $G_c(\mathbf{k}, \tau) = -\langle c_{\mathbf{k}}(\tau) c_{\mathbf{k}\sigma}^\dagger(0) \rangle$, $G_{cf}(\mathbf{k}, \tau) = -\langle c_{\mathbf{k}}(\tau) f_{\mathbf{k}\sigma}^\dagger(\tau) \rangle$ and so on. The anomalous off-diagonal members of this Green's function remind us of the Gor'kov functions in BCS theory and develop with the coherent hybridization. Using the two component notation (37), this Green's function can be written

$$\mathcal{G}_{\mathbf{k}}(\tau) = -(\partial_\tau + \underline{h}_{\mathbf{k}})^{-1} \xrightarrow{\text{F.T.}} \mathcal{G}_{\mathbf{k}}(i\omega_n) = (i\omega_n - \underline{h}_{\mathbf{k}})^{-1}, \quad (58)$$

where F.T. denotes a Fourier transform in imaginary time ($\partial_\tau \rightarrow -i\omega_n$), or more explicitly,

$$\mathcal{G}_{\mathbf{k}}(z) = (z - \underline{h}_{\mathbf{k}})^{-1} = \begin{pmatrix} z - \varepsilon_{\mathbf{k}} & -V \\ -V & z - \lambda \end{pmatrix}^{-1} = \begin{pmatrix} G_c(\mathbf{k}, z) & G_{cf}(\mathbf{k}, z) \\ G_{fc}(\mathbf{k}, z) & G_f(\mathbf{k}, z) \end{pmatrix} \quad (59)$$

$$= \frac{1}{(z - \varepsilon_{\mathbf{k}})(z - \lambda) - V^2} \begin{pmatrix} z - \lambda & V \\ V & z - \varepsilon_{\mathbf{k}} \end{pmatrix}, \quad (60)$$

where we have taken the liberty of analytically extending $i\omega_r \rightarrow z$ into the complex plane. Now we can read off the Green's functions. In particular, the hybridized conduction electron Green's function is

$$G_c(\mathbf{k}, z) = \begin{array}{c} \text{---} \\ \text{---} \\ \text{---} \end{array} \begin{array}{c} \blacktriangleright \\ \blacktriangleright \\ \blacktriangleright \end{array} = \frac{z - \lambda}{(z - \varepsilon_{\mathbf{k}})(z - \lambda) - V^2} \quad (61)$$

$$= \frac{1}{z - \varepsilon_{\mathbf{k}} - \frac{V^2}{z - \lambda}} \equiv \frac{1}{z - \varepsilon_{\mathbf{k}} - \Sigma_c(z)} \quad (62)$$

which we can interpret physically as conduction electrons scattering off resonant f -states at each site, giving rise to a momentum-conserving self-energy

$$\Sigma_c(z) = \begin{array}{c} V \\ \bullet \end{array} \text{---} \begin{array}{c} \blacktriangleright \\ \text{---} \\ \text{---} \end{array} \begin{array}{c} V \\ \bullet \end{array} = \frac{V^2}{z - \lambda}. \quad (63)$$

$O(1)$

We see that the Kondo effect has injected a resonant scattering pole at energy $z = \lambda$ into the conduction electron self-energy. This resonant scattering lies at the heart of the Kondo effect.

3.4.1 An absurd digression: the nuclear Kondo effect

The appearance of this pole in the scattering raises a vexing question in the Kondo effect: *What is the meaning of the f electron?* This might seem like a dumb question, for in electronic materials the Kondo effect certainly involves localized f electrons, and surely we can interpret this pole as the adiabatic renormalization of a hybridized band structure. This is certainly true. Yet as purists, we do have to confess that our starting model was a pure Kondo lattice model with only spin degrees of freedom: They could even have been *nuclear* spins!

This might seem absurd, yet nuclear spins do couple antiferromagnetically with conduction electrons to produce nuclear antiferromagnetism. Leaving aside practical issues of magnitude, we can learn something from the thought experiment in which the nuclear spin coupling to electrons *is* strong enough to overcome the nuclear magnetism. In this case, resonant bound states would form with the nuclear spin lattice giving rise to *charged* heavy electrons, presumably with an expanded Fermi surface.

From this line of argument we see that while it is tempting to associate the heavy fermion with a physical f or d electron localized inside the local moment, from a renormalization group perspective, the heavy electron is an emergent excitation: a fermionic bound state formed between the conduction sea and the neutral localized moments. This alternate point-of-view is useful, because it allows us to contemplate the possibility of new kinds of Kondo effects in states that are not adiabatically accessible from a band insulator or metal.

3.5 Cooper pair analogy

There is a nice analogy with superconductivity that helps one to understand the composite nature of the heavy electron. In a superconductor, electron pairs behave as loose composite bosons described by the relation

$$\overbrace{\psi_{\uparrow}(x)\psi_{\downarrow}(x')} = -F(x-x'). \quad (64)$$

Here $F(x-x') = -\langle T\psi_{\uparrow}(1)\psi_{\downarrow}(2) \rangle$ is the anomalous Gor'kov Green's function, which determines the Cooper-pair wavefunction, extended over the coherence length $\xi \sim v_F/T_c$. A similar phenomenon takes place in the Kondo effect, but here the bound state develops between spins and electrons, forming a fermion rather than a boson. For the Kondo lattice, it is perhaps more useful to think in terms of a screening time $\tau_K \sim \hbar/T_K$, rather than a length. Both the Cooper pair and heavy electron involve electrons that span decades of energy up to a cutoff, be it the Debye energy ω_D in superconductivity or the (much larger) bandwidth D in the Kondo effect [33,34].

To follow this analogy in greater depth, recall that in the path integral the Kondo interaction factorizes as

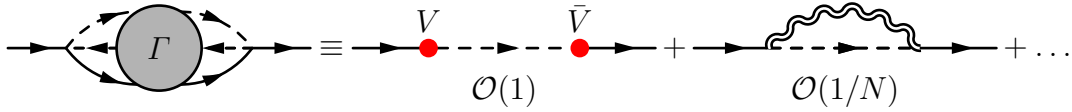
$$\frac{J}{N} c_{\beta}^{\dagger} S_{\alpha\beta} c_{\alpha} \rightarrow \bar{V} (c_{\alpha}^{\dagger} f_{\alpha}) + (f_{\alpha}^{\dagger} c_{\alpha}) V + N \frac{\bar{V}V}{J}, \quad (65)$$

so by comparing the right and left hand side, we see that the composite operators $S_{\beta\alpha}c_{\beta}$ and $c_{\beta}^{\dagger}S_{\alpha\beta}$ behave as a single fermion denoted by the contractions:

$$\frac{1}{N} \sum_{\beta} \overline{S_{\beta\alpha} c_{\beta}} = \left(\frac{\bar{V}}{J} \right) f_{\alpha}, \quad \frac{1}{N} \sum_{\beta} c_{\beta}^{\dagger} \overline{S_{\alpha\beta}} = \left(\frac{V}{J} \right) f_{\alpha}^{\dagger}, \quad (66)$$

Composite Fermion

Physically, this means that the spins bind high-energy electrons, transforming themselves into composites that then hybridize with the conduction electrons. The resulting heavy fermions can be thought of as moments ionized in the magnetically polar electron fluid to form mobile, negatively charged heavy electrons while leaving behind a positively charged ‘‘Kondo singlet.’’ Microscopically, the many-body amplitude to scatter an electron off a local moment develops a bound-state pole, which for large N we can denote by the diagrams



The leading diagram describes a kind of condensation of the hybridization field; the second and higher terms describe the smaller $\mathcal{O}(1/N)$ fluctuations around the mean-field theory.

By analogy with superconductivity, we can define a wavefunction associated with the temporal correlations between spin-flips and conduction electrons, as follows

$$\frac{1}{N} \sum_{\beta} \overline{c_{\beta}(\tau) S_{\beta\alpha}(\tau')} = g(\tau - \tau') \hat{f}_{\alpha}(\tau'), \quad (67)$$

where the spin-flip correlation function $g(\tau - \tau')$ is an analogue of the Gor'kov function, extending over a coherence time $\tau_K \sim \hbar/T_K$. Notice that in contrast to the Cooper pair, this composite object is a fermion and thus requires a distinct operator \hat{f}_{α} for its expression.

4 Heavy-fermion superconductivity

We now take a brief look at heavy-fermion superconductivity. There is a wide variety of heavy-electron superconductors, almost all of which are nodal superconductors, in which the pairing force derives from the interplay of magnetism and electron motion. In the heavy-fermion compounds, as in many other strongly correlated electron systems, superconductivity frequently develops at the border of magnetism, near the *quantum critical point* where the magnetic transition temperature has been suppressed to zero. In some of them, such as UPt_3 ($T_c=0.5\text{K}$) [35] the superconductivity develops out of a well developed heavy Fermi liquid, and in these cases, we can consider the superconductor to be paired by magnetic fluctuations within a well formed heavy Fermi liquid. However, in many other superconductors, such as UBe_{13} ($T_c=1\text{K}$) [36,37], the 115 superconductors CeCoIn_5 ($T_c=2.3\text{K}$) [38], CeRhIn_5 under pressure ($T_c=2\text{K}$) [16], NpAl_2Pd_5 ($T_c=4.5\text{K}$) [39] and PuCoGa_5 ($T_c=18.5\text{K}$) [40, 41], the superconducting transition temperature is comparable with the Kondo temperature. In many of these

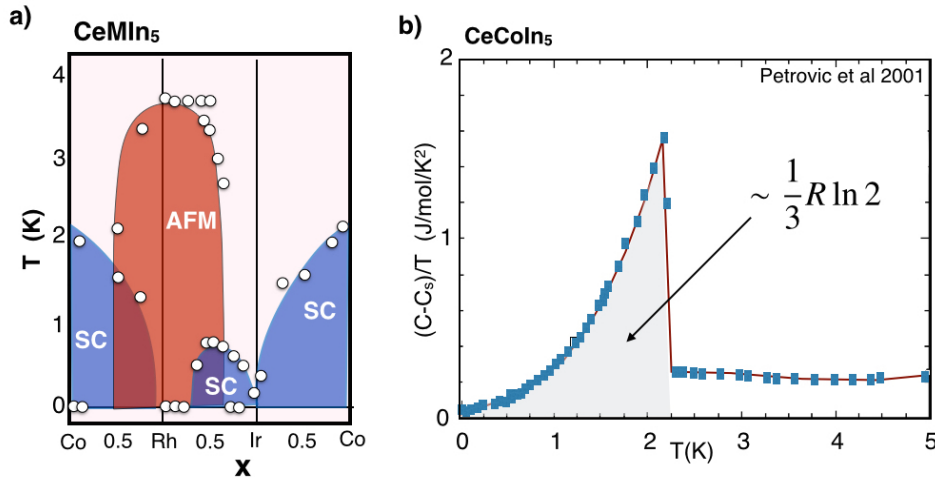


Fig. 12: (a) Phase diagram of 115 compounds $CeMIn_5$, adapted from [42], showing magnetic and superconducting phases as a function of alloy concentration. (b) Sketch of specific heat coefficient of $CeCoIn_5$, (with nuclear Schottky contribution subtracted), showing the large entropy of condensation associated with the superconducting state. (After Petrovic et al 2001 [38]).

materials, the entropy of condensation

$$S_c = \int_0^{T_c} \frac{C_V}{T} dT \quad (68)$$

can be as large as $(1/3)R \ln 2$ per rare-earth ion, indicating that the spin is in some way entangling with the conduction electrons to build the condensate. In this situation, we need to be able to consider the Kondo effect and superconductivity on an equal footing.

4.1 Symplectic spins and $SP(N)$.

Although the $SU(N)$ large- N expansion provides a very useful description of the normal state of heavy-fermion metals and Kondo insulators, there is strangely no superconducting solution. This shortcoming lies in the very structure of the $SU(N)$ group. $SU(N)$ is perfectly tailored to particle physics, where the physical excitations, the mesons and baryons, appear as color singlets, with the meson a $q\bar{q}$ quark-antiquark singlet while the baryon is an N -quark singlet $q_1 q_2 \dots q_N$, (where of course $N = 3$ in reality). In electronic condensed matter, the meson becomes a particle-hole pair, but there are no two-particle singlets in $SU(N)$ beyond $N = 2$. The origin of this failure can be traced back to the absence of a consistent definition of time-reversal symmetry in $SU(N)$ for $N > 2$. This means that singlet Cooper pairs and superconductivity can not develop at the large- N limit.

A solution to this problem that grew out of an approach developed by Read and Sachdev [43] for frustrated magnetism is to use the symplectic group $SP(N)$, where N must be an even number [44, 45]. This little-known group is a subgroup of $SU(N)$. In fact for $N = 2$, $SU(2) = SP(2)$ are identical, but they diverge for higher N . For example, $SU(4)$ has 15 generators, but its symplectic sub-group $SP(4)$ has only 10. At large N , $SP(N)$ has approximately half the number of generators of $SU(N)$. The symplectic property of the group allows it to consistently

treat time-reversal symmetry of spins, and it also allows the formation of two-particle singlets for any N .

One of the interesting aspects of $SP(N)$ spin operators is their relationship to pair operators. Consider $SP(2) \equiv SU(2)$: The pair operator is $\Psi^\dagger = f_\uparrow^\dagger f_\downarrow^\dagger$, and since this operator is a singlet, it commutes with the spin operators $[\Psi, \vec{S}] = [\Psi^\dagger, \vec{S}] = 0$, which, since Ψ and Ψ^\dagger are the generators of particle-hole transformations, implies that the $SU(2)$ spin operator is particle-hole symmetric. It is this feature that is preserved by the $SP(N)$ group, all the way out to $N \rightarrow \infty$. In fact, we can use this fact to write down $SP(N)$ spins as follows: An $SU(N)$ spin is given by $S_{\alpha\beta}^{SU(N)} = f_\alpha^\dagger f_\beta$. Under a particle-hole transformation $f_\alpha \rightarrow \text{Sgn}(\alpha) f_{-\alpha}^\dagger$. If we take the particle-hole transform of the $SU(N)$ spin and add it to itself we obtain an $SP(N)$ spin,

$$S_{\alpha\beta} = f_\alpha^\dagger f_\beta + \text{Sgn}(\alpha\beta) f_{-\beta}^\dagger f_{-\alpha}, \quad (69)$$

Symplectic Spin operator

where the values of the spin indices are $\alpha, \beta \in \{\pm 1/2, \dots, \pm N/2\}$. This spin operator commutes with the three isospin variables

$$\tau_3 = n_f - N/2, \quad \tau^+ = \sum_{\alpha>0} f_\alpha^\dagger f_{-\alpha}^\dagger, \quad \tau^- = \sum_{\alpha>0} f_{-\alpha} f_\alpha. \quad (70)$$

With these local symmetries, the spin is continuously invariant under $SU(2)$ particle-hole rotations $f_\alpha \rightarrow u f_\alpha + v \text{Sgn}(\alpha) f_{-\alpha}^\dagger$, where $|u|^2 + |v|^2 = 1$, as one can verify. To define an irreducible representation of the spin, we also have to impose a constraint on the Hilbert space, which in its simplest form is $\tau_3 = \tau^\pm = 0$, equivalent to $Q = N/2$ in the $SU(N)$ approach. In other words, the s -wave part of the f pairing must vanish identically.

4.2 Superconductivity in the Kondo-Heisenberg model

Let us take a look at the way this works in a nearest neighbor *Kondo-Heisenberg model* [46],

$$H = H_c + H_K + H_M. \quad (71)$$

Here $H_c = \sum_{\mathbf{k}\sigma} \varepsilon_{\mathbf{k}} c_{\mathbf{k}\sigma}^\dagger c_{\mathbf{k}\sigma}$ describes the conduction sea, whereas H_K and H_M are the Kondo and Heisenberg (RKKY) interactions, respectively. These take the form

$$\begin{aligned} H_K &= \frac{J_K}{N} \sum_j c_{j\alpha}^\dagger c_{j\beta} S_{\beta\alpha}(j) \rightarrow -\frac{J_K}{N} \sum_{i,j} \left((c_{j\alpha}^\dagger f_{j\alpha})(f_{j\beta}^\dagger c_{j\beta}) + \tilde{\alpha}\tilde{\beta}(c_{j\alpha}^\dagger f_{j-\alpha}^\dagger)(f_{j-\beta} c_{j\beta}) \right) \\ H_M &= \frac{J_H}{2N} \sum_{(i,j)} S_{\alpha\beta}(j) S_{\beta\alpha}(j) \rightarrow -\frac{J_H}{N} \sum_j \left[(f_{i\alpha}^\dagger f_{j\alpha})(f_{j\beta}^\dagger f_{i\beta}) + \tilde{\alpha}\tilde{\beta}(f_{i\alpha}^\dagger f_{j-\alpha}^\dagger)(f_{j-\beta} f_{i\beta}) \right] \end{aligned} \quad (72)$$

where we have introduced the notation $\tilde{\alpha} = \text{Sgn}(\alpha)$ and have shown how the interactions are expanded into particle-hole and particle-particle channels. Notice how the interactions are

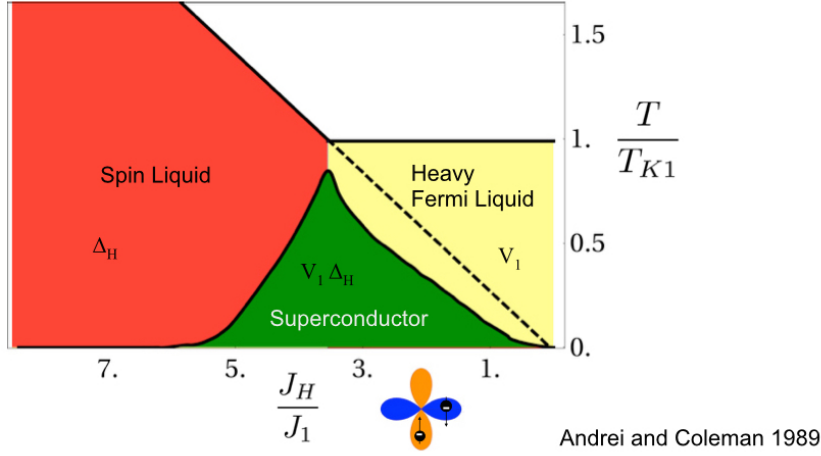


Fig. 13: Phase diagram for the two-dimensional Kondo-Heisenberg model, derived in the $SP(N)$ large- N approach, adapted from [46], courtesy Rebecca Flint.

equally divided between particle-hole and particle-particle channels. When we carry out the Hubbard-Stratonovich decoupling in each of these terms, we obtain

$$H_K \rightarrow \sum_j \left[c_{j\alpha}^\dagger \left(V_j f_{j\alpha} + \tilde{\alpha} \Delta_j^K f_{j-\alpha}^\dagger \right) + \text{H.c.} \right] + N \left(\frac{|V_j|^2 + |\Delta_j^K|^2}{J_K} \right) \quad (73)$$

$$H_H \rightarrow \sum_{(i,j)} \left[t_{ij} f_{i\alpha}^\dagger f_{j\alpha} + \Delta_{ij} \tilde{\alpha} f_{i\alpha}^\dagger f_{j-\alpha}^\dagger + \text{H.c.} \right] + N \left[\frac{|t_{ij}|^2 + |\Delta_{ij}|^2}{J_H} \right] \quad (74)$$

At each site, we can always rotate the f electrons in particle-hole space to remove the Kondo pairing component and set $\Delta_j^K = 0$, but the pairing terms in the Heisenberg component can not be eliminated. This mean-field theory describes a kind of *Kondo-stabilized spin-liquid* [46]. The physical picture is as follows: In practice, a spin-liquid is unstable to magnetism, but its happy coexistence with the Kondo effect brings its energy below that of the antiferromagnet. The hybridization of the f with the conduction sea converts the spinons of the spin liquid into charged fermions. The t_{ij} terms describe various kind of exotic density waves. The Δ_{ij} terms now describe pairing amongst the composite fermions.

To develop a simple theory of the superconducting state, we restrict our attention to uniform, static saddle points, dropping the t_{ij} . Let us look at the resulting mean-field theory. In two dimensions, this becomes

$$H = \sum_{\mathbf{k}, \alpha > 0} (\tilde{c}_{\mathbf{k}\alpha}^\dagger, \tilde{f}_{\mathbf{k}\alpha}^\dagger) \begin{bmatrix} \varepsilon_{\mathbf{k}} \tau_3 & V \tau_1 \\ V \tau_1 & \vec{w} \cdot \vec{\tau} + \Delta_{H\mathbf{k}} \tau_1 \end{bmatrix} \begin{pmatrix} \tilde{c}_{\mathbf{k}\alpha} \\ \tilde{f}_{\mathbf{k}\alpha} \end{pmatrix} + \mathcal{N}_s N \left(\frac{|V|^2}{J_K} + 2 \frac{|\Delta_H|^2}{J_H} \right) \quad (75)$$

where

$$\tilde{c}_{\mathbf{k}\alpha}^\dagger = (c_{\mathbf{k}\alpha}^\dagger, \tilde{\alpha} c_{-\mathbf{k}, -\alpha}), \quad \tilde{f}_{\mathbf{k}\alpha}^\dagger = (f_{\mathbf{k}\alpha}^\dagger, \tilde{\alpha} f_{-\mathbf{k}, -\alpha}) \quad (76)$$

are Nambu spinors for the conduction and f -electrons. The vector \vec{W} of Lagrange multipliers couples to the isospin of the f electrons: Stationarity of the free energy with respect to this variable imposes the mean-field constraint $\langle \tilde{f}^\dagger \vec{\tau} f \rangle = 0$. The function $\Delta_{H\mathbf{k}} = \Delta_{\mathbf{k}} (\cos k_x -$

$\cos k_y$) is the f -electron pair wavefunction. Here we have chosen a d -wave form-factor. For this choice, the local f pair density automatically vanishes and so we need only choose $\vec{w} = (0, 0, \lambda)$, where λ couples to τ_3 (imposing the constraint $n_f = N/2$). We could have also tried an extended s -wave pair wavefunction, but in this case, the induced s -wave pair density becomes finite, and the effect of the \vec{w} constraint is to suppress the transition temperature. By seeking stationary points in the free energy with respect to variations in Δ_H , V , and λ one can derive the phase diagram for d -wave pairing, shown in Fig. 13. The mean-field theory shows that superconductivity develops at the interface between the Fermi liquid and the spin liquid.

5 Topological Kondo insulators

One of the areas of fascinating development in the last few years is the discovery that Kondo insulators can develop *topological order* to form a *topological Kondo insulator*. Topological order refers to the idea that a quantum mechanical ground state can develop a non-trivial topology. One of the defining features of topological ground states is the development of protected surface states. The best known example of topological order is the integer quantum Hall effect, where an integer-filled Landau level develops topological order that is responsible for the robust quantization of the quantum Hall effect [47–49]. In a remarkable series of discoveries in 2006, [50–57] it became clear that strong spin-orbit coupling can play the role of a synthetic magnetic field, so that band insulators can also develop a non-trivial topology while preserving time-reversal symmetry. Such Z_2 topological band insulators are defined by a single topological $Z_2 = \pm 1$ index that is positive in conventional insulators, but reverses in topological Z_2 insulators. This topological feature manifests itself through the formation of robust conducting surface states.

In 2007, Liang Fu and Charles Kane showed that if an insulator has both time-reversal and inversion symmetry [57], this Z_2 index is uniquely determined by the parities δ_{in} of the Bloch states at the high-symmetry points Γ_i of the valence band

$$Z_2 = \prod_{\Gamma_i} \delta(\Gamma_i) = \begin{cases} +1 & \text{conventional insulator} \\ -1 & \text{topological insulator} \end{cases} \quad (77)$$

Fu Kane formula for the Z_2 index of topological insulators

where $\delta(\Gamma_i) = \prod_n \delta_{in}$ is the product of the parities of the occupied bands at the high-symmetry points in the Brillouin zone. This formula allows one to determine whether an insulator state is topological merely by checking whether the index $Z_2 = -1$, without a detailed knowledge of the ground-state wavefunction.

It used to be thought that Kondo insulators could be regarded as “renormalized silicon.” The discovery of topological insulators forced a reevaluation of this viewpoint. The large spin-orbit coupling and the odd parity of the f states led to the proposal, by Dzero, Sun, Galitski, and the author [58], that Kondo insulators can become topologically ordered. The Fu-Kane formula has

a special significance for Kondo insulators, which contain *odd parity* f electrons hybridizing with *even parity* d electrons. Each time an f electron crosses through the band gap, exchanging with a conduction d state, this changes the Z_2 index, making it highly likely that certain Kondo insulators are topological. The oldest known Kondo insulator SmB_6 , discovered almost 50 years ago, was well known to possess a mysterious low-temperature conductivity plateau [59, 60], and the idea that this system might be a topological Kondo insulator provided an exciting way of explaining this old mystery. The recent observation of robust [61, 62] conducting surface states in the oldest Kondo insulator SmB_6 supports one of the key elements of this prediction, prompting a revival of interest in Kondo insulators as a new route for studying the interplay of strong interactions and topological order.

SmB_6 is really a mixed-valent system, which takes us a little beyond the scope of this lecture. One of the other issues with SmB_6 is that its local crystal field configuration is likely to be a Γ_8 quartet state [63] rather than a Kramers doublet. Nevertheless, key elements of its putative topological Kondo insulating state are nicely illustrated by a *spin-orbit coupled* Kondo-Heisenberg model, describing the interaction of Kramers doublet f states with a d band. The model is essentially identical to (Eq. (71))

$$H = \sum_{\mathbf{k}\sigma} \varepsilon_{\mathbf{k}} \psi_{\mathbf{k}\sigma}^\dagger c_{\mathbf{k}\sigma} + J_K \sum_j \psi_{j\alpha}^\dagger \psi_{j\beta} S_{\beta\alpha}(j) + J_H \sum_{i,j} S_{\alpha\beta}(i) S_{\beta\alpha}(j) \quad (78)$$

with an important modification that takes into account the large spin-orbit coupling and the odd parity of the f states. This forces the local Wannier states $\Psi_{j\alpha}$ that exchange spin with the local moment to be odd-parity combinations of nearest-neighbor conduction electrons, given by

$$\psi_{j\alpha}^\dagger = \sum_{i,\sigma} c_{i\sigma}^\dagger \Phi_{\sigma\alpha}(\mathbf{R}_i - \mathbf{R}_j). \quad (79)$$

We will consider a simplified model with the form factor

$$\Phi(\mathbf{R}) = \begin{cases} -i\hat{R} \cdot \frac{\vec{\sigma}}{2}, & \mathbf{R} \in \text{n.n} \\ 0 & \text{otherwise.} \end{cases} \quad (80)$$

This form factor describes the spin-orbit mixing between states with orbital angular momentum l differing by one, such as f and d or p and s orbitals. The odd parity of the form-factor $\Phi(\mathbf{R}) = -\Phi(-\mathbf{R})$ derives from the odd-parity f orbitals, while the prefactor $-i$ ensures that the hybridization is invariant under time reversal. The Fourier transform of this form factor, $\Phi(\mathbf{k}) = \sum_{\mathbf{R}} \Phi(\mathbf{R}) e^{i\mathbf{k}\cdot\mathbf{R}}$ is then

$$\Phi(\mathbf{k}) = \vec{s}_{\mathbf{k}} \cdot \vec{\sigma} \quad (81)$$

where the vector $\vec{s}_{\mathbf{k}} = (\sin k_1, \sin k_2, \sin k_3)$ is the periodic equivalent of the unit momentum vector $\hat{\mathbf{k}}$. Notice how $\vec{s}(\Gamma_i) = 0$ vanishes at the high symmetry points.

The resulting mean-field Hamiltonian takes the form

$$H_{TKI} = \sum_{\mathbf{k}} \psi_{\mathbf{k}}^\dagger h(\mathbf{k}) \psi_{\mathbf{k}} + \mathcal{N}_s \left[\left(\frac{V^2}{J_K} + \frac{3t^2}{J_H} - \lambda Q \right) \right], \quad (82)$$

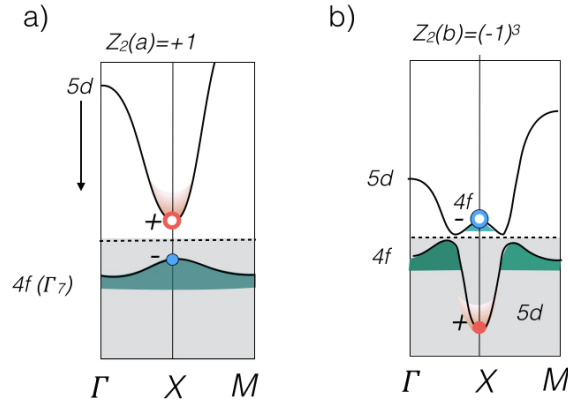


Fig. 14: (a) When the d band is above the filled f band, a trivial insulator is formed. (b) When the d band crosses the f band at the three X -points, the Z_2 parity changes sign, giving rise to a topological insulator.

where $\psi_{\mathbf{k}}^\dagger = (c_{\mathbf{k}\sigma}^\dagger, f_{\mathbf{k}\sigma}^\dagger)$ and

$$h(\mathbf{k}) = \begin{pmatrix} \varepsilon_{\mathbf{k}} & V\vec{\sigma} \cdot \vec{s}_{\mathbf{k}} \\ V\vec{\sigma} \cdot \vec{s}_{\mathbf{k}} & \varepsilon_{f\mathbf{k}} \end{pmatrix} \quad (83)$$

while $\varepsilon_{f\mathbf{k}} = 2t_f(c_x + c_y + c_z) + \lambda$ ($c_l \equiv \cos k_l$) is the dispersion of the f state resulting from a mean-field decoupling of the intersite Heisenberg coupling in the particle-hole channel. For small \mathbf{k} , the hybridization in the Hamiltonian $h(\mathbf{k})$ takes the form $V\vec{\sigma} \cdot \mathbf{k}$, closely resembling the topologically non-trivial triplet p -wave gap structure of superfluid He-3B. Like He-3B, the hybridization only develops at low temperatures, making SmB_6 an adaptive insulator.

Let us for the moment treat $h(\mathbf{k})$ as a rigid band structure. Suppose the f band were initially completely filled, with a completely empty d band above it (See Fig. 14a). This situation corresponds to a conventional band insulator with $Z_2 = +1$. Next, let us lower the d conduction band until the two bands cross at a high symmetry point, causing the gap to close and then to re-open. We know, from de Haas-van Alphen studies of the iso-electronic material LaB_6 [64] (whose band-structure is identical to SmB_6 but lacks the magnetic f electrons) and from ARPES studies [65–67] that in SmB_6 the d band crosses through the Fermi surface at the three X points. Once the d band is lowered through the f band around the three X points, the odd-parity f states at the X point move up into the conduction band, to be replaced by even-parity d states. This changes the sign of $Z_2 \rightarrow (-1)^3 = -1$, producing a topological ground state. Moreover, since there are three crossings, we expect there to be three spin-polarized surface Dirac cones.

We end by noting that at the time of writing, our understanding of the physics SmB_6 is in rapid flux on both the experimental and theoretical front. Spin-resolved ARPES [68] measurements have detected the presence of spin textures in the surface Fermi surfaces around the surface \bar{X} point, a strong sign of topologically protected surface states. Two recent theoretical works [69, 70] have shown that the spin textures seen in these experiments are consistent with a spin-quartet ground state in SmB_6 . Despite this progress, consensus on the topological nature of SmB_6 has not yet been achieved, and competing groups have offered alternate interpretations of the data, including the possibility of polarity-driven surface metallicity [71] and Rashba-split surface states, both of a non-topological origin [72]. Another area of experimental controversy

concerns the possible de Haas-van Alphen oscillations created by surface topological excitations, with one report of the detection of surface de Haas-van Alphen signals [73] and a recent, very remarkable report of *bulk* de Haas-van Alphen signals associated with unhybridized, quantum critical d electrons [74].

6 Coexisting magnetism and Kondo effect

In this short lecture, I have given a quick introduction to the paramagnetic phases of heavy-fermion systems. One of the major open questions in heavy-fermion and Kondo-lattice physics concerns the physics of magnetism and the right way to describe the development of magnetism within these materials. There is growing evidence that magnetism and the Kondo effect can coexist, sometimes homogeneously and sometimes inhomogeneously. For example, in the 115 superconductor CeRhIn₅ there is evidence for a microscopic and homogeneous coexistence of local-moment magnetism and heavy-fermion superconductivity under pressure [75]. By contrast, in the geometrically frustrated CePdAl [76,77], two thirds of the Cerium sites spontaneously develop magnetism, leaving the other third to undergo a Kondo effect [78]. What is the right way to describe these coexistent states? One possibility that I have worked on with Aline Ramires [79, 80] is the use of a *supersymmetric* representation of the spin

$$S_{\alpha\beta} = f_{\alpha}^{\dagger} f_{\beta} + b_{\alpha}^{\dagger} b_{\beta} \quad (84)$$

where the f_{α}^{\dagger} and b_{α}^{\dagger} are fermionic and bosonic creation operators. Such a representation permits in principle, the existence of *two-fluid* ground states, involving a Gutzwiller projection of bosonic and fermionic wavefunctions

$$|\Psi\rangle = P_G |\Psi_F\rangle |\Psi_B\rangle, \quad (85)$$

where $|\Psi_F\rangle$ is the fermionic component of the wavefunction describing the Kondo-quenched local moments, while $|\Psi_B\rangle$ describes the formation of long-range magnetic correlations within a bosonic RVB wavefunction, and

$$P_G = \int \prod_j \frac{d\theta_j}{2\pi} e^{i\theta_j(n_B+n_F-1)} \quad (86)$$

is a Gutzwiller projection operator onto the state with one spin per site. We have been trying to describe such mixed-state wavefunctions in the large- N limit, seeking saddle-point solutions where a bosonic and fermionic fluid coexist [80]. One of the ideas that emerges from this kind of approach is the possibility that the soft modes at a quantum critical point might develop fermionic character, a kind of emergent supersymmetry [81].

Acknowledgment

This article was written with the support of the National Science Foundation under grant no NSF DMR-1309929.

References

- [1] P. Coleman: *Handbook of Magnetism and Advanced Magnetic Materials* (John Wiley and Sons, Amsterdam, 2007), Vol. 1, pp. 95–148
- [2] P. Coleman: *Introduction to Many-Body Physics* (Cambridge University Press, 2015)
- [3] J.L. Smith and E.A. Kmetko, *Journal of the Less Common Metals* **90**, 83 (1983)
- [4] P.W. Anderson, *Phys. Rev.* **115**, 2 (1959)
- [5] P.W. Anderson, *Phys. Rev.* **124**, 41 (1961)
- [6] J. Kondo, *Prog. Theor. Phys.* **32**, 37 (1964)
- [7] R.H. White and T.H. Geballe in: H. Ehrenreich, F. Seitz, and D. Turnbull (eds.): *Solid State Physics* (Academic Press, New York, 1979), Vol. 15, p. 283
- [8] M.D. Daybell: In G. Rado and H. Suhl (Eds.) *Magnetism* (Academic Press, New York, 1973), Vol. 5, p. 121
- [9] N. Mott, *Philosophical Magazine* **30**, 403 (1974)
- [10] S. Doniach, *Physica*, **91 B+C**, 231 (1977)
- [11] M.A. Ruderman and C. Kittel, *Phys. Rev* **96**, 99 (1954)
- [12] T. Kasuya, *Prog. Theo. Phys.* **16**, 45 (1956)
- [13] K. Yosida, *Phys. Rev.* **106**, 896 (1957)
- [14] T. Kasuya, *Prog. Theor. Phys.* **16**, 45 (1956)
- [15] R. Jullien, J. Fields, and S. Doniach, *Phys. Rev. B* **16**, 4889 (1977)
- [16] T. Park, F. Ronning, H.Q. Yuan, M.B. Salmon, R. Movshovich, J.L. Sarrao, and J.D. Thompson, *Nature* **440**, 65 (2006)
- [17] P. Coleman, C. Pépin, Q. Si, and R. Ramazashvili, *J. Phys. Cond. Matt.* **13**, 273 (2001)
- [18] H. v.Löhneysen, A. Rosch, M. Vojta, and P. Wölfle, *Rev. Mod. Phys.* **79**, 1015 (2007)
- [19] A. Menth, E. Buehler, and T.H. Geballe, *Phys. Rev. Lett* **22**, 295 (1969)
- [20] G. Aeppli and Z. Fisk, *Comm. Condens. Matter Phys.* **16**, 155 (1992)
- [21] Z. Fisk, J.L. Sarrao, S.L. Cooper, P. Nyhus, G.S. Boebinger, A. Passner, and P.C. Canfield, *Physica B* **223-224**, 409 (1996)
- [22] H. Tsunetsugu, M. Sigrist, and K. Ueda, *Rev. Mod. Phys.* **69**, 809 (1997)

- [23] P. Riseborough, *Adv. Phys.* **49**, 257 (2000)
- [24] P.W. Anderson: *Valence Fluctuations in Solids* (North Holland, Amsterdam, 1981)
- [25] P. Coleman, *Phys. Rev.* **28**, 5255 (1983)
- [26] N. Read and D. Newns, *J. Phys. C* **16**, 3274 (1983)
- [27] P. Coleman, *Phys. Rev. B* **29**, 3035 (1984)
- [28] N. Read and D.M. Newns, *J. Phys. C* **29**, L1055 (1983)
- [29] A. Auerbach and K. Levin, *Phys. Rev. Lett.* **57**, 877 (1986)
- [30] A.J. Millis, and P.A. Lee, *Phys. Rev. B* **35**, 3394 (1987)
- [31] P. Coleman, *Phys. Rev. B* **35**, 5072 (1987)
- [32] B. Coqblin and J.R. Schrieffer, *Phys. Rev.* **185**, 847 (1969)
- [33] S. Burdin, A. Georges, and D.R. Grempel, *Phys. Rev. Lett* **85**, 1048 (2000)
- [34] T.A. Costi and N. Manini, *Journal of Low Temperature Physics* **126**, 835 (2002)
- [35] G.R. Stewart, Z. Fisk, J.O. Willis, and J.L. Smith, *Phys. Rev. Lett* **52**, 679 (1984)
- [36] H.R. Ott, H. Rudigier, Z. Fisk, and J.L. Smith, *Phys. Rev. Lett* **50**, 1595 (1983)
- [37] H.R. Ott, H. Rudigier, T.M. Rice, K. Ueda, Z. Fisk, and J.L. Smith, *Phys. Rev. Lett* **52**, 1915 (1984)
- [38] C. Petrovic, P.G. Pagliuso, M.F. Hundley, R. Movshovich, J.L. Sarrao, J.D. Thompson, Z. Fisk, and P. Monthoux, *J. Phys. Cond. Matt* **13**, L337 (2001)
- [39] D. Aoki, Y. Haga, T. Matsuda, N. Tateiwa, S. Ikeda, and *et al.*, *Journal of The Physical Society of Japan* (2007)
- [40] J.L. Sarrao, L.A. Morales, J.D. Thompson, B.L. Scott, G.R. Stewart, F. Wastin, J. Rebizant, P. Boulet, E. Colineau, and G.H. Lander, *Nature* (2002)
- [41] N.J. Curro, T. Caldwell, E.D. Bauer, L.A. Morales, M.J. Graf, Y. Bang, A.V. Balatsky, J.D. Thompson, and J.L. Sarrao, *Nature* **434**, 622 (2005)
- [42] J.L. Sarrao and J.D. Thompson, *Journal of the Physical Society of Japan* **76**, 051013 (2007)
- [43] N. Read and S. Sachdev, *Phys. Rev. Lett* **66**, 1773 (1991)
- [44] R. Flint, M. Dzero, P. Coleman, and M. Dzero, *Nature Physics* **4**, 643 (2008)

- [45] R. Flint and P. Coleman, *Phys. Rev. Lett.* **105**, 246404 (2010)
- [46] P. Coleman and N. Andrei, *J. Phys. Cond. Matt.* **C 1**, 4057 (1989)
- [47] R.B. Laughlin, *Phys. Rev.* **B23**, 5632 (1981)
- [48] D. Thouless, M. Kohmoto, M. Nightingale, and M. Den Nijs, *Phys. Rev. Lett.* **49**, 405 (1982)
- [49] F.D.M. Haldane, *Phys. Rev. Lett.* **61**, 2015 (1988)
- [50] C.L. Kane and E.J. Mele, *Phys. Rev. Lett.* **95**, 146802 (2005)
- [51] B.A. Bernevig, T.L. Hughes, and S.-C. Zhang, *Science* **314**, 1757 (2006)
- [52] J.E. Moore and L. Balents, *Phys. Rev. B* **75**, 121306(R) (2007)
- [53] R. Roy, *Phys. Rev. B* **79**, 195321 (2009)
- [54] L. Fu, C.L. Kane, and E.J. Mele, *Phys. Rev. Lett.* **98**, 106803 (2007)
- [55] M. König, S. Wiedmann, C. Brüne, A. Roth, H. Buhmann, L.W. Molenkamp, X.-L. Qi, and S.-C. Zhang, *Science* **318**, 766 (2007)
- [56] D. Hsieh, D. Qian, L. Wray, Y. Xia, Y.S. Hor, R.J. Cava, and M.Z. Hasan, *Nature* **452**, 970 (2008)
- [57] L. Fu and C. Kane, *Physical Review B* **76**, 45302 (2007)
- [58] M. Dzero, K. Sun, V. Galitski, and P. Coleman, *Phys. Rev. Lett.* **104**, 106408 (2010)
- [59] J.W. Allen, B. Batlogg, and P. Wachter, *Phys. Rev. B* **20**, 4807 (1979)
- [60] J.C. Cooley, M.C. Aronson, A. Lacerda, Z. Fisk, P.C. Canfield, and R.P. Guertin, *Phys. Rev. B* **52**, 7322 (1995)
- [61] S. Wolgast, C. Kurdak, K. Sun, J.W. Allen, D.-J. Kim, and Z. Fisk, *Phys. Rev. B* **88**, 180405 (2013)
- [62] D. J. S. Thomas, T. Grant, J. Botimer, Z. Fisk, and J. Xia, *Scientific Reports* **3**, 3150 (2014)
- [63] V. Alexandrov, M. Dzero, and P. Coleman, *Phys. Rev. Lett.* **111**, 226403 (2013)
- [64] Z. Fisk, A.J. Arko, J.B. Ketterson, G. Crabtree, F.M. Mueller, L.R. Windmiller, and D. Karim, *Phys. Rev. B* **13**, 5240 (1976)
- [65] M. Neupane, N. Alidoust, S.Y. Xu, and T. Kondo, *Nat. Commun.* **4**, 2991 (2013)

- [66] N. Xu, X. Shi, P.K. Biswas, C.E. Matt, R.S. Dhaka, Y. Huang, N.C. Plumb, M. Radović, J.H. Dil, E. Pomjakushina, K. Conder, A. Amato, Z. Salman, D.M. Paul, J. Mesot, H. Ding, and M. Shi, *Phys. Rev. B* **88**, 121102 (2013)
- [67] J.D. Denlinger, J.W. Allen, J.-S. Kang, K. Sun, B.-I. Min, D.-J. Kim, and Z. Fisk, arXiv:1312.6636v2 (2013)
- [68] N. Xu, P.K. Biswas, J.H. Dil, R.S. Dhaka, G. Landolt, S. Muff, C.E. Matt, X. Shi, N.C. Plumb, M.R. Cacute, E. Pomjakushina, K. Conder, A. Amato, S.V. Borisenko, R. Yu, H.M. Weng, Z. Fang, X. Dai, J. Mesot, H. Ding, and M. Shi, *Nat. Commun.* **5**, 1 (2014)
- [69] M. Legner, A. Rüegg, and M. Sigrist, arXiv:1505.02987v1 (2015)
- [70] P.P. Baruselli and M. Vojta, arXiv:1505.03507v1 (2015)
- [71] Z.-H. Zhu, A. Nicolaou, G. Levy, N.P. Butch, P. Syers, X.F. Wang, J. Paglione, G.A. Sawatzky, I.S. Elfimov, and A. Damascelli, *Phys. Rev. Lett.* **111**, 216402 (2013)
- [72] P. Hlawenka, K. Siemensemeyer, E. Weschke, A. Varykhalov, J. Sánchez-Barriga, N.Y. Shitsevalova, A.V. Dukhnenko, V.B. Filipov, S. Gabáni, K. Flachbart, O. Rader, and E.D.L. Rienks, arXiv:1502.01542 (2015)
- [73] G. Li, Z. Xiang, F. Yu, T. Asaba, B. Lawson, P. Cai, C. Tinsman, A. Berkley, S. Wolgast, Y.S. Eo, D.-J. Kim, Ç. Kurdak, J.W. Allen, K. Sun, X.H. Chen, Y.Y. Wang, Z. Fisk, and L. Li, *Science* **346**, 1208 (2014)
- [74] B.S. Tan, Y.T. Hsu, B. Zeng, M.C. Hatnean, N. Harrison, Z. Zhu, M. Hartstein, M. Kiourlappou, A. Srivastava, M.D. Johannes, T.P. Murphy, J.H. Park, L. Balicas, G.G. Lonzarich, G. Balakrishnan, and S.E. Sebastian, *Science* **349**, 287 (2015)
- [75] G. Knebel, D. Aoki, D. Braithwaite, B. Salce, and J. Flouquet, *Phys. Rev. B* **74**, 020501 (2006)
- [76] A. Donni, G. Ehlers, H. Maletta, P. Fischer, H. Kitazawa, and M. Zolliker, *J. Phys.: Condens. Matter* **8**, 11213 (1996)
- [77] C. Dolores Nunez-Regueriro, M. LaCroix and B. Canals, *Physica C* **282-287**, 1885 (1997)
- [78] V. Fritsch, N. Bagrets, G. Goll, W. Kittler, M. J. Wolf, K. Grube, C.-L. Huang, and H. v.Löhneysen, *Phys. Rev. B* **89**, 054416 (2014)
- [79] P. Coleman, C. Pépin, and A.M. Tsvelik, *Phys. Rev. B* **62**, 3852 (2000)
- [80] A. Ramires and P. Coleman, To be published (2015)
- [81] S.-S. Lee, *Phys. Rev. B* **76**, 075103 (2007)